University of Turin

Doctoral School in Life and Health Sciences

PhD. course of Medical Pathophysiology

XXX cycle

Protective Role of Stem Cell Derived Extracellular Vesicles in an *in vitro* Model of Hyperglycemia-Induced Endothelial Injury

Coordinator:

Prof. Franco Veglio

Scientific Supervisor:

Prof. Giovanni Camussi

Candidate:

Chiara Gai

ACADEMIC YEAR 2017/2018

SUMMARY

Abstract 1

Introduction 3

Extracellular Vesicles 3

Biogenesis and cargo 4

Mechanism of action 6

Mesenchymal stem cells 8

MSC derived EVs 10

ASC derived EVs 11

Hyperglycemia and endothelial damage 12

Diabetic nephropathy 13

Objectives 14

Materials and methods 15

Cell cultures 15

Isolation and Characterization of EVs from ASC and MSC 15

Western Blot Analysis 16

Real Time PCR 17

BrdU Proliferation Assay 17

Annexin V Apoptosis Assay 18

Oxidative Stress Analysis 18

Matrigel Angiogenesis Assay 19

MiRNA Array Profile 19

Protein Array Profile 20

Pathway and Gene Ontology Analysis of EV Content 21

Statistical Analysis 21

Results 23

EV characterization 23

Hyperglycemic model set-up 24
EVs counteract hyperglycemia-induced damages on proliferation and apoptosis 26
EVs counteract hyperglycemia-induced oxidative stress 28
EVs restore angiogenesis after hyperglycemia-induced damage 30
ASC and MSC EVs carry a common subset of miRNAs involved in angiogenesis and cell proliferation 32
ASC and MSC EVs carry a common subset of proteins involved in cell proliferation and apoptosis 34
ASC EVs miRNA and protein cargo targets common pathways involved in angiogenesis, cell motility and cell proliferation 36
MSC EVs miRNA and protein cargo targets common pathways involved in cell proliferation, and endothelial cell migration 38
Discussion 41
Conclusions 45
References 46

ABSTRACT

Background

Adipose and bone marrow-derived mesenchymal stem cells are two populations of multipotent adult stem cells with immunosuppressive, anti-inflammatory, and regenerative properties. It has been previously described that extracellular vesicles (EVs) derived from stem cells possess pro-regenerative and pro-angiogenic abilities. Hyperglycemia is a pathological condition affecting diabetic patients. Long-term effects of hyperglycemia are endothelial dysfunction and vascular lesions leading to diabetic microangiopathy.

The aim of the present study was to evaluate whether stem cell-derived EVs woul inhibit endothelial cells microangiopathy-like dysfunctions induced by hyperglycemia. The second objective was to perform a bioinformatic analysis of the miRNA and protein content of stem cell-derived EVs in order to identify molecules involved in their biological effect.

Methods

We set up an *in vitro* hyperglycemic model by culturing human microvascular endothelial cells in hyperglycemic constant or intermittent conditions for 7 days, to mimic a chronic damage. At day 5, endothelial cells were incubated with adipose and mesenchymal stem cell-derived EVs or vehicle alone for 48 hr. At day 7, we evaluated apoptosis, oxidative stress, and capillary-like formation ability on Matrigel. Finally, we analyzed EV miRNA and protein cargo and performed a bioinformatic analysis.

Results

Intermittent and constant high glucose models significantly decreased endothelial cell proliferation, increased the percentage of apoptotic cells, promoted oxidation of intracellular proteins, and reduced capillary-like structure formation. Treatment with both kinds of EVs significantly restored proliferation, inhibited apoptosis and oxidation, and restored capillary-like formation. Protein and miRNA carried by EVs significantly target pathways involved in cell cycle and proliferation, motility and angiogenesis, and apoptosis.

Conclusions

The results of the present study demonstrate that adipose and bone marrow mesenchymal stem cell-derived EVs may inhibit the endothelial dysfunction induced by high glucose concentration, which mimics diabetic microvascular injury. Probably, these effects are due to the transfer of their miRNA and protein cargo to recipient cells.

INTRODUCTION

Extracellular vesicles

Extracellular vesicles (EVs) are defined as a heterogeneous set of secreted membrane vesicles. This group includes exosomes and vesicles that are indicated in the literature with different names, such as ectosomes, microvesicles or shedding vesicles. EVs are composed by a phospholipid bilayer that contains or encloses lipid raft-interacting proteins, surface receptors, cytoplasmic proteins, and nucleic acids [1]. It has been widely proven that EVs confer stability to enclosed proteins and nucleic acids by protecting them from enzymatic degradation, and mediate the entry into specific recipient cell types [2-5]. Moreover, EV encapsulation of nucleic acids, including mRNA, long and small non-coding RNA (lncRNA, miRNA, tRNA), and in some instances DNA, were found to protect from enzymatic degradation and to allow exchange of genetic information among cells [6-9]. Some transmembrane proteins are common to all EVs, while other are cell-specific and represent a signature of the cell of origin. Moreover, EV content may vary depending on the metabolic and activation state of the cells [10]. Since their discovery roughly 30 years ago [11-13], EVs were purified from virtually all mammalian cell types and body fluids, and even from lower eukaryotes, prokaryotes, and plants [14]. This suggests that EV-mediated cell signaling emerged very early during evolution as a primitive and essential mechanism of cell communication [15].

Biogenesis and cargo

Based on their biogenesis, EVs can be classified in two different groups: microvesicles and exosomes. **Microvesicles** are a heterogeneous population of vesicles larger than exosomes. They originate by budding and shedding from cell surface [16-18]. Changes in the composition in lipids, proteins and other components of the plasma membrane (PM) modify the curvature of the membrane and facilitate the budding of microvesicles. This process is regulated, at least in part, by the interaction of proteins, such as arrestin domain-containing protein-1 (ARRDC1) with the late endosomal protein TSG101. Microvesicles fission is due to the dynamic contraction of the plasma membrane induced by myosin and actin cytoskeletal rearrangements. The process is regulated by Ras-related GTPase ADP-ribosylation factor 6 (ARF6) and its signaling cascade [19, 20]. Moreover, calcium level impacts on specific enzymes, including flippase, floppase, and scramblase, which modify the asymmetry of PM phospholipids [21]. Elevated calcium levels promote the transfer of phosphatydilserine (PS) towards the inner membrane by inhibiting flippase. This process is ATP-dependent [22] and activates scramblase leading the shift of PS from the inner to the outer leaflet of the cell membrane [23]. The activation of cytosolic proteases, such as gelsolin and calpain, by calcium promotes the detachment of PM protrusions from cortical actin [24].

Exosomes show a variable size ranging approximately from 40 to 150 nm [1]. They are formed by budding of the membrane into the lumen of multivesicular bodies (MVB), which are part of the endocytic pathway. Exosomes are stored within MVBs of the late endosome until MVBs fuse with the PM and release their content [16, 25, 26]. Several proteins are involved with the formation of exosomes, such as the

components of the Endosomal Sorting Complex Required for Transport (ESCRT) machinery and the accessory proteins TSG101, ALIX and VPS4 [27]. Nevertheless, other ESCRT-independent mechanisms have been described [28]. The docking of MVB with the PM is mediated by several components of the RAB family of small GTPase proteins (RAB2B, RAB5A, RAB7, RAB9A, RAB11, RAB27A, RAB27B, RAB35 [29] and RLP-1 [30]). Some members of the tetraspanin family, such as CD63, CD81, CD9, are enriched in exosomes and have been recognized as exosome markers [29]. On the other hand, specific markers for microvesicles are lacking and it is difficult to discriminate EVs basing on biomarkers. Moreover, even if the biogenesis of microvesicles and exosomes is based on different processes, some mechanisms and proteins seem to be shared [31].

Evidence shows that EV content varies depending on originating cell and biogenesis mechanism, however the compartmentalization of proteins and RNA is, at least in part, a regulated process. Comparative lipidomic, proteomic and transcriptomic analyses usually find an enrichment of subsets of lipids, proteins or RNAs in EVs compared with their cells of origin [31-35]. Several proteins involved in EV biogenesis were shown to regulate compartmentalization into EV. For example, ESCRT complex recruits proteins into both exosomes and microvesicles [36]. ALIX has been shown to be associated with Ago2, a member of the Argonaute protein family, which binds miRNAs. The complex ALIX-Ago2-miRNAs has been found in exosomes isolated from human liver stem cells (HLSC) [37]. Another work showed that breast cancer exosomes contain functional AGO2-associated miRNAs, which are mature and induce transcriptome alterations in target cells [38]. The heterogeneous nuclear ribonucleoprotein A2B1 (hnRNPA2B1) was shown to

recognize specific motifs and regulate miRNA loading into exosomes [39]. The RNA-binding protein Y-box protein I (YBX1) binds to miR-223 and is necessary for its packaging into exosomes [40]. In colorectal cancer cells, KRAS seems to mediate miRNA sorting into exosomes [41] by regulating Ago2 secretion [42]. Increasing reports show that EVs are particularly enriched in other types of small RNAs, such as tRNA fragments, yRNA, vault RNAs, miRNAs fragments [43-45]. The presence of a regulated mechanism of small RNA sorting into exosomes has been observed also in Leishmania, confirming that it is conserved throughout evolution [46]. However, the biological functions of small RNAs found in EVs are not completely clear, while the miRNA and/or their activity are widely studied in several pathologies.

Despite their differences in origin and size, these two major classes of EVs display similar functions. Specifically, they transfer, from one cell to another, cellular constituents that may account for an extension of the functional properties of originating cells. For simplicity, the term EVs will be used to refer collectively to exosomes and microvesicles.

Mechanism of action

Once released from the cell of origin, EVs may remain in the extracellular space and interact with recipient cells in a paracrine fashion or may be degraded. Otherwise, vesicles may migrate far from the site of origin by entering into biological fluids, like blood, saliva, urine, and many others [24].

EVs interact with target cells through various mechanisms. It has been proposed that the uptake may occur by receptor-mediated interactions leading to endocytosis. Many surface molecules may mediate exosome uptake. For example,

P-selectin glycoprotein ligand-1 expressed by macrophage-derived EVs mediates binding to platelets [24], phosphatidylserine receptors favor entry into macrophages [47] and heparan sulfate proteoglycans induce vesicle capture in many cell types [48]. EVs derived from proangiogenic progenitors present on their membrane α4 and β1 integrins and L-selectin, which interact with and mediate the uptake by recipient endothelial cells [7]. Recently, syncytin-1, which belongs to a family of mammalian fusogens, has been implicated in the cell uptake of placental EVs [49].

Another way of internalization is direct fusion of EVs with cell PM through a receptor-independent mechanism. Indeed, EVs can entry by clathrin-dependent endocytic mechanisms, as micropinocytosis, caveolin-mediated internalization, phagocytosis, and lipid raft–mediated uptake [50].

Recently, evidence has highlighted that EV composition and microenvironmental conditions may influence EV uptake. For example, it was demonstrated that a high lipid raft content in EVs facilitates their fusion with cells [50, 51] and lipid rafts are involved in EV uptake in the kidney [52]. In addition, acidic pH in the extracellular environment enhances EV-membrane fusion [51, 53], and, in tumors, the acidic microenvironment promotes the release of EVs with higher cell fusion capacity [53]. A recent work has shown that the uptake of T lymphocyte-derived EVs by human retinal endothelial cells is regulated by either temperature, extracellular calcium, and the expression levels of the low-density lipoprotein receptor (LDLR) [54]. However, it is still unclear whether different interaction mechanisms coexist in the same cell or if they vary depending on recipient cell type and EV origin.

Through fusion with target cells, EVs may convey receptors and adhesion molecules that exert an active role in recipient cells. For instance, platelet-derived EVs can transfer the CD41 ligand to endothelial cells [55] or to tumor cells [56] with consequent enhancement of their pro-adhesive properties. Moreover, EVs can deliver mRNA and miRNA [8, 57, 58], which may undergo translation into protein or regulate gene expression [15, 59, 60]. This hypothesis is supported by studies based on lipid fusion assays, which observed that the transfer of miRNAs shuttled by EVs to dendritic cells (DCs) depends both on actin-mediated phagocytosis and on the fusion of cholesterol-rich plasma membrane microdomain [53, 61]. Moreover, some recent interesting studies have used Cre recombinase technique [62-64] or a combination of fluorescent and bioluminescent reporters tagging EV membrane and RNA molecules [65] to demonstrate that mRNAs are transferred from cell to cell by EVs *in vivo*.

However, internalization is not always necessary for transmission of signals. Indeed, another mechanism of communication is based on direct cell stimulation. For instance, platelet-derived EVs may directly activate intracellular signaling pathways in endothelial [55], inflammatory [66] and human hematopoietic cells [6], thus favoring tumor invasion and diffusion.

Mesenchymal stem cells

Mesenchymal stem cells (MSCs) are non-hematopoietic pluripotent progenitor cells capable of differentiate into multiple mesoderm-type cell lineages (osteoblasts, chondrocytes, adipocytes, and endothelial cells), but also in non-mesoderm-type lineage (neuronal-like cells) [67]. MSCs can be isolated from bone

marrow, umbilical cord blood, and adipose tissue [68]. Isolation protocol of MSCs is easily reproducible and MSCs showed a large differentiation potential, so they are the first stem cell types introduced into the clinic [67]. In 2006, the Society for Cellular Therapy proposed a set of criteria to define MSCs. They should show: plastic adherence; positivity for specific sets of cell surface markers, such as CD73, CD90, CD105; and the ability to differentiate *in vitro* into adipocytes, chondrocytes and osteoblasts [69].

MSCs have shown promising regenerative, immunosuppressive, and anti-inflammatory properties, so they have emerged as a potential tool for tissue repair and wound healing in regenerative medicine, but their mechanism of action is not completely understood [70]. It was previously believed that MSCs transplanted into injured tissues could differentiate into various cell types and so regenerate the tissue. Then it was observed that the therapeutic effects were mainly due to the paracrine activity of MSCs, which leads to the activation of protective mechanisms and to the stimulation of self-renewal and endogenous regeneration [71].

The paracrine activity of MSCs is mainly based on the release of immunomodulators, angiogenic factors, anti-apoptotic factors, antioxidants molecules, and cellular chemotaxis inducers. These factors are important to reduce tissue damage and to regulate the innate and the adaptive immune responses [72]. MSCs can also inhibit several T-lymphocyte activities, to stimulate the production of regulatory T cells, and to alter the cytokine production of dendritic cells, effector T cells, and natural killer cells, resulting in a more anti-inflammatory phenotype [71].

Because of their characteristics, MSCs have been suggested as promising candidates for a variety of therapeutic applications, such as the treatment of immune disorders, neurological diseases, hepatic injury, acute renal failure, and myocardial infarction [72].

Adipose Mesenchymal Stem Cells (ASCs) can be easily isolated from subcutaneous adipose tissue using a minimally invasive liposuction and can be used for autologous transplantation without graft-versus-host reaction. Thus, ASCs have become a very attractive stem cell source for regenerative medicine. Indeed, as well as MSCs, ASCs have shown a regenerative potential in various diseases, so they may both be used in regenerative medicine [73].

In recent years, EVs were recognized as a novel mechanism of paracrine communication through which MSCs and ASCs may, at least in part, exert their regenerative activity [70].

MSC-derived EVs

EVs were shown to transfer several paracrine signaling molecules, such as immunomodulators, angiogenic factors, anti-apoptotic factors, antioxidants molecules, and cellular chemotaxis inducers [72]. Recent studies have demonstrated that EVs derived from MSC (MSC EVs) contain vascular endothelial growth factor (VEGF), transforming growth factor β1 (TGF-β1), interleukin 8 (IL-8) [74,75], hepatocyte growth factor (HGF) [76-78], HES family BHLH transcription factor 1 (HES1) [79], and human T-cell factor 4 (TCF4) [80-81], but also pro-angiogenic miRNAs, such as miR-210, miR-126, miR-132, miR-21 [82], miR-222, let-7f, and miRNA stimulating cell-cycle progression and proliferation, such as miR-

191, miR-222, miR-21, let- 7a [83, 84]. These factors induce survival, proliferation, and proangiogenic signaling in recipient endothelial cells [72].

ASC-derived EVs

Recent evidence shows that EVs derived from ASCs (ASC EVs) contain several angiogenic factors, such as milk fat globule-EGF factor 8 protein (MFGE8), angiopoietin like 1 (ANGPTL1), and thrombopoietin [10]. Moreover, they carry matrix metalloproteinases (MMPs) that play an important role in angiogenesis by facilitating endothelial cell migration and by promoting activation of angiogenic growth factors and other signaling molecules [85]. It has also been shown that the proangiogenic content of ASC EVs is modulated by the microenvironment, for example *in vitro* by the addition of different growth factors [86], or *in vivo* by obesity, which reduces their pro-angiogenic potential [87].

EVs were identified as a candidate substitute for stem cells in regenerative medicine, since they can reduce safety risks, such as de-differentiation, tumorigenesis, or immune response activation due to cell transplantation [70]. Several studies have explored the regenerative properties of MSC EVs in different diseases. It was demonstrated that MSC EVs are able to reduce infarct size, to enhance tissue repair, and to increase angiogenesis in cardiovascular diseases [70]. They promote tubule-epithelial regeneration and reduce tubular cell apoptosis, fibrosis, and tubular atrophy in a model of acute kidney injury (AKI) [70]. A recent study has reported that MSC EVs induce functional recovery in AKI through the transfer of miRNA [88]. MSC EVs have been shown to be effective in a model of renal ischemia reperfusion injury, with a reduction of cell apoptosis, increased proliferation and angiogenesis, amelioration of histological lesions [89]. MSC EVs

can also promote wound healing by inducing proliferation and migration of fibroblasts and by enhancing angiogenesis, both *in vitro* [90] and *in vivo* [91].

Hyperglycemia and endothelial damage

Diabetes mellitus is a metabolic disease spread worldwide with a high and growing prevalence. It is characterized by a complete deficiency of insulin due to pancreatic insufficiency (type 1 diabetes) or by insulin resistance in peripheral tissues, with a reduced glucose uptake rate during insulin exposure (type 2 diabetes). Hyperglycemia occurs in both kind of diabetes mellitus and is a leading cause of several functional alterations in vascular endothelium, especially in type 1 diabetes, in which chronic hyperglycemia strongly affects endothelium homeostasis [92]. A first decrease in the production of vasodilators (i.e. nitric oxide) and/or an increased production of vasoconstrictors (i.e. endothelin), together with mitochondrial collapse and the consequent increased generation of oxygen-derived radicals (ROS), impair endothelium-dependent vasodilation [93]. This cause an increased permeability to macromolecules. Moreover, von Willebrand factor level rises, leading to increased prethrombotic and procoagulant activity. E-selectin and vascular cell adhesion molecule 1 (v-CAM1) level rises, favoring increased adhesion and permeability to leucocytes. The recruitment of leucocytes promotes inflammation and release of proinflammatory cytokines, such as tumor necrosis factor (TNF)-α, interleukin (IL)-6, soluble CD40L, soluble ICAM, soluble E-selectin, soluble lectin-like oxidized low-density lipoprotein receptor-1, monocyte chemoattractant protein, and high-sensitivity C-reactive protein. Lastly, extracellular matrix synthesis intensifies, due to the proliferation of vascular

smooth muscle cells, and the deposition of fibronectin and type IV collagen fragments increases. Therefore, the accumulation of matrix proteins leads to basal membrane thickening, [94]. Taken together, these factors end up causing disruption of the endothelial barriers, impaired vessel wall turnover and abnormal vascular remodeling [95].

Diabetic microangiopathy affects capillaries and thus damages particularly renal, retinal, and neuronal capillaries, with consequent nephropathy, retinopathy, and neuropathy.

Diabetic nephropathy

Diabetic nephropathy is characterized by an abnormal extracellular matrix (ECM) accumulation within mesangial cells. The activation of the local renin-angiotensin system triggers an upregulation of TGF-β [95], and proinflammatory and profibrotic signals from glomerular cells and infiltrating macrophages cause mesangial expansion. The thickening of the glomerular capillary basal membrane leads to the impairment of the glomerular filtration barrier with regression of the cytoplasmic extensions of podocytes. These events lead to albuminuria, which is the most important early clinical risk factor for diabetic nephropathy. The most advanced pathological change is the glomerulosclerosis, which derives from the apoptosis of podocytes and glomerular endothelial cells [96].

The exact pathological mechanisms leading to diabetic microangiopathy are complex and not completely clear. Even if it is evident that glucose, at least in early stages, plays a major role in the changes of vessel permeability. The understanding of these processes may help treatment of the microvessel disease, which affects many diabetic patients worldwide.

OBJECTIVES

The aim of the present study was to evaluate the potential protective role of ASCs and MSC EVs in an *in vitro* model of microvascular endothelial injury that recapitulates the chronic hyperglycemic conditions that lead to microvascular dysregulation in diabetic patients. Moreover, we comparatively analyzed miRNA and protein content of ASCs and MSC EVs and performed a bioinformatic analysis in the attempt to identify molecules involved in the observed protective effect of EVs.

MATERIALS AND METHODS

Cell Cultures

Human microvascular endothelial cells (HMEC) were obtained through immortalization of primary human dermal microvascular endothelial cells with simian virus 40 [97, 98]; the cells were cultured as previously described [99]. HMEC cultured in normal glucose Endothelial Basal Medium (EBM, Lonza) were used as control (CTR). Glucose concentration of EBM was 5.6 mM. High glucose- and high mannitol-EBM were obtained by adjusting EBM to 28 mM of α-D-glucose (Sigma Aldrich) or 28 mM of mannitol (Sigma Aldrich). Constant hyperglycemic (HG) model was performed by culturing HMEC in high glucose-EBM for 7 days. Intermittent hyperglycemic (INT HG) model was performed by culturing HMEC in 48 hr alternated cycles of high glucose-EBM, or high mannitol-EBM as osmotic control, and normal glucose-EBM, for 7 days.

Human ASCs and MSCs (Lonza) were cultured in Mesenchymal Stem Cell Basal Medium (MSCBM, Lonza) supplemented with MSC-GM kit (Lonza) and 1% Antibiotic Antimycotic solution (Sigma-Aldrich) at 37°C in 5% CO2 incubator. ASCs and MSCs were grown until confluent, and sub-cultured and characterized as previously described [10]. Cells at passages 4 to 6 were used for the experiments.

Isolation and Characterization of EVs from ASC and MSC

ASCs and MSCs were starved for 16 hours. Supernatants were collected and EVs were isolated by differential ultracentrifugation as previously described [10]. The quality of EVs preparation was evaluated on the basis of their morphology and

expression of exosome markers as follow. Quantification and size distribution of EVs was performed using NanoSight LM10 (NanoSight Ltd) equipped with nanoparticle tracking analysis NTA 2.3 analytic software [100]. Transmission electron microscopy was performed on EVs purified from MSCs and ASCs and observed through Jeol JEM 1010 electron microscope as previously described [37].

Western Blot Analysis

Cells were lysed at 4°C for 20 minutes in a RIPA lysis buffer supplemented with 1% PMSF, 1% Protease Inhibitor Cocktail, 1% Phosphatase Inhibitor Cocktail 1, and 1% Phosphatase Inhibitor Cocktail 3 (Sigma Aldrich). The lysate was centrifuged at 12,000 x g for 20 minutes at 4°C to precipitate and discard cellular debris. The protein content of the supernatants was measured by Bradford. Aliquots, containing 30 μg of protein of the cell lysates, were subjected to 10% sodium dodecyl sulfate-polyacrylamide gel electrophoresis under reducing conditions and electroblotted onto nitrocellulose membrane filters. The membranes were blocked with 5% nonfat milk in 20 mmol/L Tris-HCl, pH 7.5, 500 mmol/L NaCl plus 0.1% Tween (TBS-T) and immunoblotted overnight at 4°C with the relevant primary antibodies at the appropriate concentration: CD63, Alix, Actin, VEGF, v-CAM-1 (Santa Cruz Biotechnology), CD9 and Fibronectin (Abcam). After extensive washings with TBS-T, the blots were incubated for 2 hours at room temperature with peroxidase-conjugated isotype-specific secondary antibodies (Pierce, Thermo Fisher Scientific), washed with PBS-T. The protein bands were visualized with Clarity Western ECL Substrate (Bio-Rad) and ChemiDoc™ XRS+ System (Bio-Rad). The average density of each band was measured by Quantity One Analysis Software

(Bio-Rad), normalized for the average density of the respective actin band. The mean normalized density of at least 4 experiments is expressed as fold change over CTR.

Real Time PCR

Total RNA was extracted by TriZol reagent (Life Technologies, Thermo Fisher Scientific) according to manufacturer's instructions. cDNA was produced from total RNA using the High Capacity cDNA Reverse Transcription Kit (Applied Biosystems, Thermo Fisher Scientific). Briefly, 200 ng mRNA, 2 µl RT buffer, 0.8 µl dNTP mixture, 2 µl RT random primers, 1 µl MultiScribe reverse transcriptase, and 4.2 µl nuclease-free water were used for each cDNA synthesis. Twenty microliters of RT-PCR mix, containing 1X SYBR GREEN PCR Master Mix (Applied Biosystems, Thermo Fisher Scientific), 100 nM of each primer (VEGF or GAPDH), were analyzed using a 48-well StepOne Real Time System (Applied Biosystems, Thermo Fisher Scientific). Negative cDNA controls (no cDNA) were cycled in parallel with each run.

BrdU Proliferation Assay

HMEC at 5 days of HG or INT HG conditioning were seeded at 2,000 cells/well into 96-well plates with AF in EBM medium (adjusted or not to 28 mM glucose) and left to adhere. After 4 hr, cell medium was changed with DMEM (Euroclone), adjusted or not to 28 mM glucose and supplemented with 10% ultra-centrifuged fetal bovine serum (FBS, Thermo Fisher Scientific). FBS was ultra-centrifuged for 8 hr to remove EVs. Then, cells were treated with EVs from ASCs or MSCs at the dose of 10,000 EVs/cell. DNA synthesis was detected as incorporation of 5-bromo-2′-deoxyuridine (BrdU) into the cellular DNA using an ELISA kit (Roche), following the

manufacturer's instructions. Optical density was measured with an ELISA reader (Bio-Rad) at 405 nm.

Annexin V Apoptosis Assay

HMEC at day 5 of hyperglycemic conditioning were plated on 24-well plates at a density of 2×10^4 cells/well in EBM medium (adjusted or not to 28 mM glucose) and left to adhere. Then, cell medium was changed with DMEM (Euroclone), adjusted or not to 28 mM glucose and supplemented with 10% EV-deprived FBS (Thermo Fisher Scientific). Cells were treated with EVs from ASCs or MSCs at the dose of 10^4 EVs/cell. At day 7 of hyperglycemic conditioning, cells were washed with PBS and harvested with 1% trypsin. Supernatant, PBS used for washing and cells were collected by centrifugation at 400 × g for 5 min. After removal of the supernatant, cells were resuspended in 100 μl of DMEM. Then 100 μl of Muse Annexin V & Dead Cell Kit reagent (Merck-Millipore) was added to each sample, cells were mixed and incubated at RT for 20 minutes in the dark. Qualitative and quantitative assessments of apoptosis were conducted with a Muse Cell analyzer (Merck Millipore).

Oxidative Stress Analysis

HMEC at day 5 of hyperglycemic conditioning were plated on 8-well chamber slides (Thermo Fisher Scientific) at a density of 10^4 cells/well with AF in EBM medium (adjusted or not to 28 mM glucose) and left to adhere. Then, cell medium was changed with DMEM (Euroclone) adjusted or not to 28 mM glucose and supplemented with 10% ultra-centrifuged FBS (Thermo Fisher Scientific). Cells were treated with EVs from ASCs or MSCs at the dose of 10^4 EVs/cell. At day 7 of

hyperglycemic conditioning, cells were washed with PBS, fixed with ice-cold methanol and protein carbonyls generated by oxidative stress were labelled with 2,4-dinitrophenylhydrazine (DNPH) from OxyICC kit (Merck Millipore), according with manufacturer's instructions. DNPH was detected by a peroxidase-conjugated antibody and streptavidin was used as substrate. Nuclei were stained with DAPI. All reagents were provided by OxyICC kit (Merck Millipore). The immunodetection was performed by a fluorescent confocal microscope (Zeiss) at 60x magnification. Fluorescence intensity was measured by ImageJ 1.49v software (NIH) and Corrected Total Cell Fluorescence (CTCF) was calculated as previously described [101, 102].

Matrigel Angiogenesis Assay

In vitro formation of capillary-like structures was studied on growth factor-reduced Matrigel (Corning). To evaluate the formation of capillary-like structures, HMECs were washed twice with PBS, detached with 1% trypsin, and seeded (2×10^4 cells/well) onto Matrigel-coated wells in DMEM supplemented with 10% ultra-centrifuged FBS and adjusted or not to 28 mM of glucose, in the presence or absence of EVs from ASCs or MSCs (10^4 EVs/cell). After 24 hr, cells were observed with a Nikon-inverted microscope (10X) and photographed with a Leica-digital camera. Image analysis was performed automatically with the Angiogenesis Analyzer tool by ImageJ 1.49v software (NIH).

MiRNA Array Profile

EVs isolated from three different MSCs and ASCs preparations were analyzed for their miRNA content by quantitative real time (qRT) PCR using the Applied

Biosystems TaqMan MicroRNA Assay Human Panel Early Access kit (Life Technologies), able to profile 754 human mature miRNAs by sequential steps of reverse transcription (Megaplex RT Pools; Life Technologies) using an Applied Biosystems 7900H qRT-PCR instrument. Briefly, single stranded cDNA was generated from total RNA sample (80 ng) by reverse transcription using a mixture of looped primers (Megaplex RT kit, Life Technologies) following manufacturer's protocol. The pre-amplification reaction for each sample was performed using a TaqMan® PreAmp Master Mix 2X (Life Technologies) mixed with specific Megaplex™ PreAmp Primers (10X) (Life Technologies). Pre-amplified products were then diluted, loaded in the TaqMan MicroRNA Array and qRT-PCR experiments were performed.

Raw Ct values, automatic baseline and threshold were calculated using the SDS software version 2.3. Comparison of miRNA expression was conducted using the Expression Suite software (Life Technologies). Fold change (Rq) in miRNA expression among the three samples was calculated as $2^{-\Delta Ct}$ and data were normalized using global normalization algorithm [103]. Values of Ct > 35 or Amp score < 0.7 was excluded from analysis.

Protein Array Profile

Purified EVs from MSCs and ASCs were lysed in 1 ml of 2× Cell Lysis Buffer (RayBiotech), and aliquots (1 mg of EV protein) were used for RayBio Biotin Label-based Human Antibody Array 1000 (RayBiotech) that was performed according to the manufacturer instructions. The array provides detection of 1000 proteins. The biotin-conjugated antibodies on each membrane served as positive controls. Data

analysis was conducted after background signal subtraction and normalization to positive controls (Mean background +4 standard deviations, accuracy ≈ 99%). Comparison of signal intensities among array images was used to define relative differences in expression levels of each sample. The arrays were performed in duplicates, using two different MSC and ASC EVs preparations. Only proteins detected in both preparations were mentioned as consistently detected. Among these, only proteins with a normalized signal intensity above the average of all detected proteins were used for the analysis.

Pathway and Gene Ontology Analysis of EV Content

Target prediction and Kyoto Encyclopedia of Gene and Genomes (KEGG) biological pathway enrichment analysis for miRNA enriched in MSC and ASC EVs was performed by FunRich V3 [104] and the web-based program DIANA-mirPath V3 [105], with miRNA targets searched on validated target database TarBase v7.0. Results were merged by "pathway-union" criteria. The p value was calculated by DIANA online software with False Discovery Rate (FDR) correction, p value threshold at 0.05 and MicroT threshold at 0.8. Fisher's exact test was used as the enrichment analysis method. For protein class analysis and pathway classification, Panther classification system was used (http://pantherdb.org/). Gene Ontology (GO) analysis was conducted using Enrichr online software [106, 107].

Statistical Analysis

Statistical analysis was performed using GraphPad Prism 6.01 Software. Proliferation (BrdU), apoptosis (Annexin V), oxidative stress (DNPH), and tube formation assay (Matrigel) were analyzed using Ordinary One Way Anova test,

significance was calculated by Fisher's LSD test. Western Blot data were analyzed using nonparametric Kruskal-Wallis test. For Real Time PCR data analysis, Excel software (Microsoft Office 365 ProPlus) was used to calculate ΔCt, -ΔΔCt, and RQ. Statistical analysis was performed on RQ values by GraphPad Prism 6.01 software using nonparametric Kruskal-Wallis test. We considered differences to be statistically significant when $p<0.05$. At least 4 experiments for each assay were performed with similar results. Data are expressed as mean ± SEM.

RESULTS

EV characterization

As shown in figure 1, EVs released from ASCs and MSCs showed comparable size and concentration, as seen by NanoSight. The size was similar also by transmission electron microscopy, but ASC EVs were less homogeneous then MSC EVs (Fig. 1 inset). By western blot, both EVs expressed the exosome marker CD63.

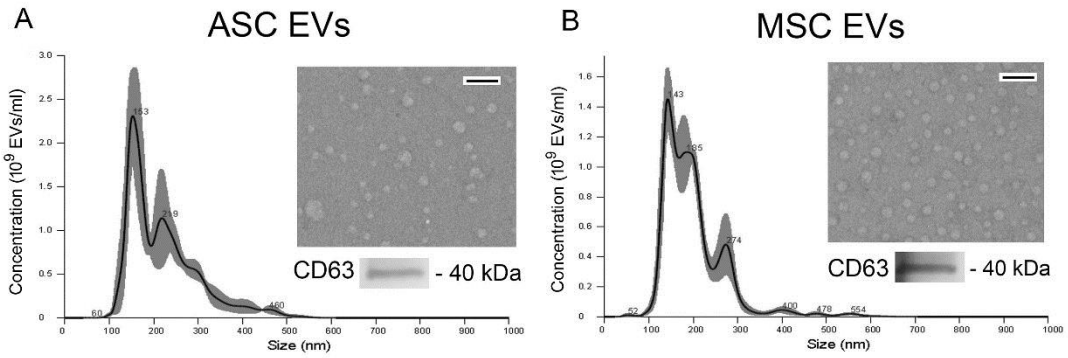

Figure 1: Characterization of ASC and MSC EVs.
Representative NanoSight analysis of ASC (A) and MSC (B) EVs showing concentration of particles (10^9 EVs/ml) and size (nm). Insets show transmission electron microscopy of EVs negatively stained with NanoVan. EVs were viewed using a JEOL Jem 1010 electron microscope (original magnification x75,000, black line= 200 nm). Representative western blot analysis of EVs purified by differential ultracentrifugation showing the expression of the exosome marker CD63.

Hyperglycemic model set-up

In order to test the protective role of stem cell-derived EVs, we set up an *in vitro* hyperglycemic model of endothelial injury. We chose to condition cells with a glucose level comparable to glycemic concentration measurable in diabetic patients. Cells were conditioned for 7 days in order to mimic a chronic damage. HMECs were cultured in constant high glucose (HG), or in intermittent high glucose (INT HG), which mimic glucose peaks occurring in diabetic patients. Figure 2A shows the experimental condition. HMECs cultured with a normal glucose concentration were used as control (CTR) and HMECs cultured with constant high mannitol (HM) concentration were used as osmotic control. HMECs were treated with EVs at day 5.

As shown in figure 2C and D, differences in the expression of some endothelial markers were observed after hyperglycemic conditioning. Western blot analysis showed significantly higher level of fibronectin (Fig. 2C) and v-CAM1 (Fig. 2D) protein in both HG and INT HG conditions compared to CTR. On the contrary, VEGF protein level was significantly lower in HMEC in HG and INT HG conditions, compared to NG condition (Fig. 2E). This was confirmed by Real Time PCR, which showed a reduction in the transcript of VEGF-A isoform in HG condition and a significant reduction in INT HG condition, compared to CTR (Fig. 2B).

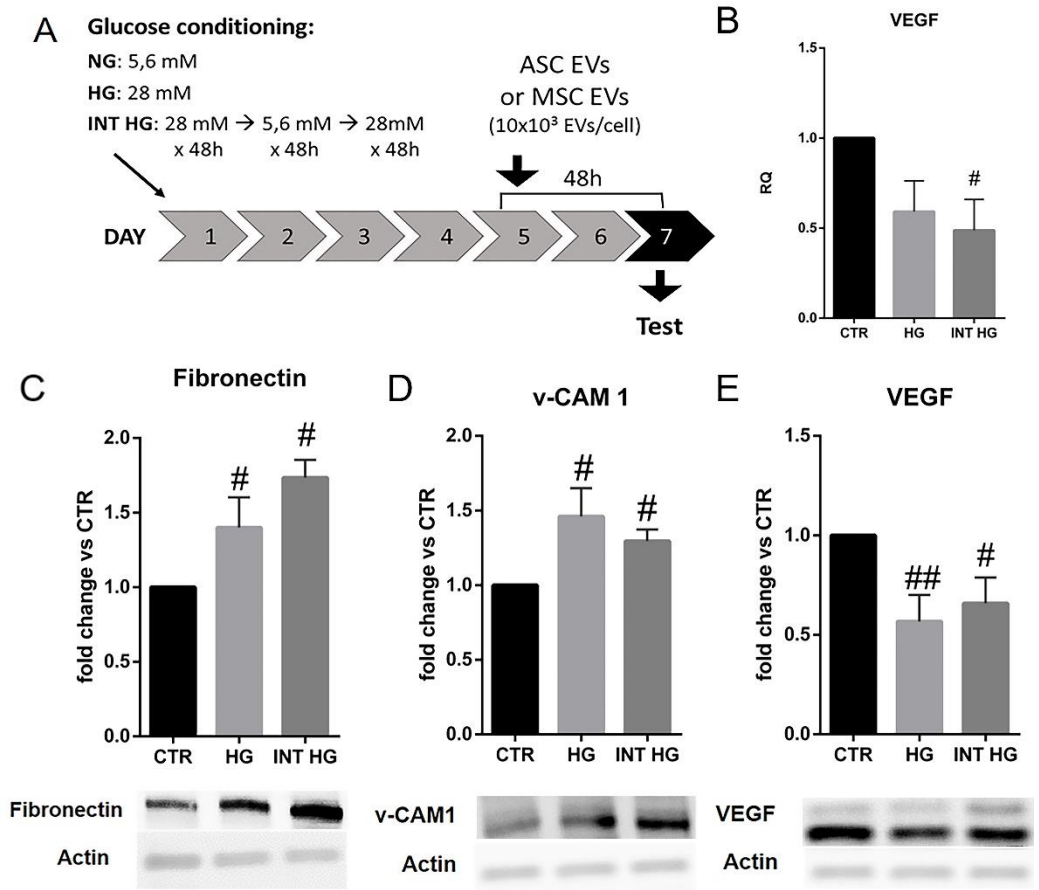

Figure 2: Set up of *in vitro* hyperglycemic model of endothelial injury

The scheme summarizes glucose concentration and time points of cell conditioning with high glucose media for setting up the model and dose and time of EV treatment (A). Real Time PCR for VEGF transcript in both HG and INT HG conditions is expressed as Relative Quantification (RQ) on CTR. GAPDH was used as endogenous control (B). Representative western blot for fibronectin (C), v-CAM1 (D), and VEGF (E) are shown. The intensity of each band was quantified and normalized for Actin. The mean of n≥4 experiments is shown and expressed as fold change vs CTR. All histograms represent mean ± SEM. # p ≤ 0,05 and ## p ≤ 0,01 for HG/INT HG vs CTR.

EVs counteract hyperglycemia-induced damages on proliferation and apoptosis

We performed proliferation and apoptosis assays to understand whether high glucose affects proliferation and survival of endothelial cells and whether ASC and MSC EVs exert a protective role from high glucose damages. As shown in figure 3, BrdU incorporation in dividing cells was significantly reduced in both HG (Fig. 3A) and INT HG (Fig. 3B) conditions, compared to CTR.

After a 48 hr treatment with ASC and MSC EVs, the proliferation was significantly increased in both HG (Fig. 3A) and INT HG (Fig. 3B) conditions, compared to untreated HG- or INT HG-conditioned cells. EVs from ASCs were less effective then MSC EVs (Fig. 3A, B). Proliferation was not affected by HM conditioning.

By Annexin V apoptosis assay, we observed that the percentage of living cells was significantly reduced in HG condition compared to CTR. EVs showed a protective effect (Fig. 3C). The percentage of dead cells was also significantly increased in HG condition, and reduced after EV treatment. EVs from MSCs showed a stronger anti-apoptotic effect compared to ASC EVs (Fig. 3D). Also in INT HG model, the percentage of live cells was significantly reduced (Fig. 3E) and the percentage of dead cells was significantly increased (Fig. 3F). Treatment with both ASC and MSC EVs significantly reverted INT HG effects (Fig. 3E, F) compared to untreated INT HG cells. In the INT HG model, the anti-apoptotic potential of the two types of EVs was comparable.

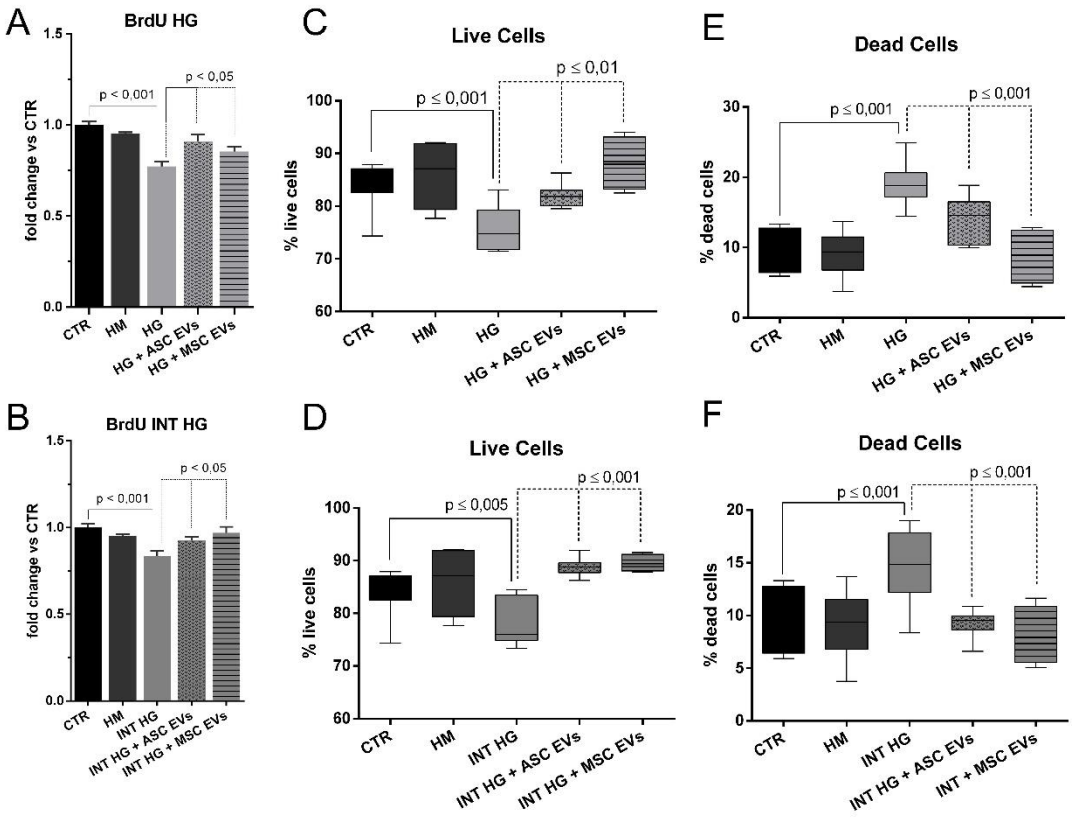

Figure 3: Pro-proliferative and anti-apoptotic effects of ASC and MSC EVs

BrdU proliferation assay for HG (A) and INT HG (B) models. Histograms (A, B) shows mean ± SEM of n=5 experiments expressed as fold change vs CTR. Annexin V apoptosis assay (C-F) showed the percentage of live cells in HG (C) and INT HG (D) models and also percentage of dead cells in HG (E) and INT HG (F) models. The boxes in plots (C-F) show 10-90 percentile, whiskers represent min to max value; n=4 experiments were performed for each data-set. The statistical significance was calculated comparing HG/INT HG vs CTR and HG/INT HG + EVs vs HG/INT HG.

EVs counteract hyperglycemia-induced oxidative stress

We evaluated the levels of oxidized proteins in the hyperglycemic model. We observed that the oxidative stress was remarkably increased in HG (Fig. 4C) and INT HG (Fig. 4D), but not in HM (Fig. 4B) condition compared to CTR (Fig. 4A). The quantitative analysis of cell fluorescence intensity (CTCF) confirmed that the increased protein oxidation was statistically significant in both HG (Fig. 4I) and INT HG (Fig. 4J) conditions. After the treatment with ASC (Fig. 4E, F) and MSC (Fig. 4G, H) EVs, we observed a significant decrease of the oxidative stress in both hyperglycemic conditions. The measurement of the mean fluorescence intensity confirmed that the reduction of oxidized protein after EV treatment was statistically significant in both HG (Fig. 4I) and INT HG (Fig. 4J) models.

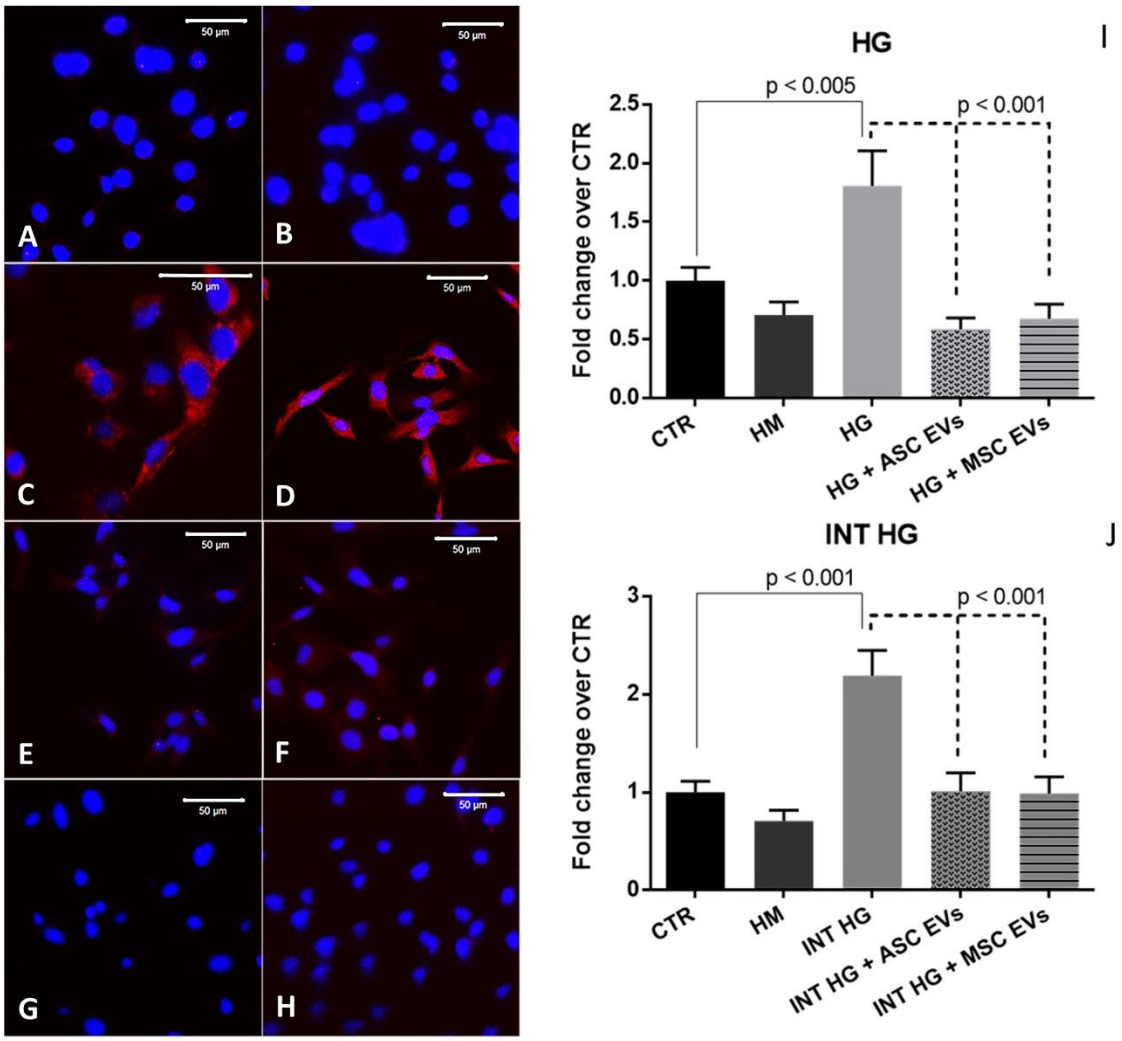

Figure 4: Anti-oxidant activity of ASC and MSC EVs

Representative images of immunofluorescent staining of nuclei with DAPI (blue) and oxidized proteins with 2,4-DNPH (red) of CTR (A), HM (B), HG (C), INT HG (D), HG + ASC EVs (E), INT HG + ASC EVs (F), HG + MSC EVs (G), INT HG + MSC EVs (H). Scale bars in the upper-right corner of each photograph indicate 50 µm. Pictures were taken by Zeiss fluorescent confocal microscope at 60x magnification. Histograms show the mean CTCF ± SEM expressed as fold change over CTR for HG (I) and INT HG (J) models. N=4 experiments were performed for each data set. The statistical significance was calculated comparing HG/INT HG vs CTR and HG/INT HG + EVs vs HG/INT HG.

EVs restore angiogenesis after hyperglycemia-induced damage

We investigated the capability of endothelial cells to form capillary-like structures in high glucose conditions in Matrigel. In fact, HMECs in CTR (Fig. 5A) and HM (Fig. 5B) spontaneously form vessel-like structures. We observed that HMECs in HG (Fig. 5C) and INT HG (Fig. 5D) partially lost this ability. In both HG and INT HG conditions, total length of capillary-like structures was significantly reduced compared to CTR, while HM condition was comparable to CTR. As shown in figure 5, the treatment with ASC and MSC EVs significantly increased the number of vessel-like structures in both HG and INT HG models.

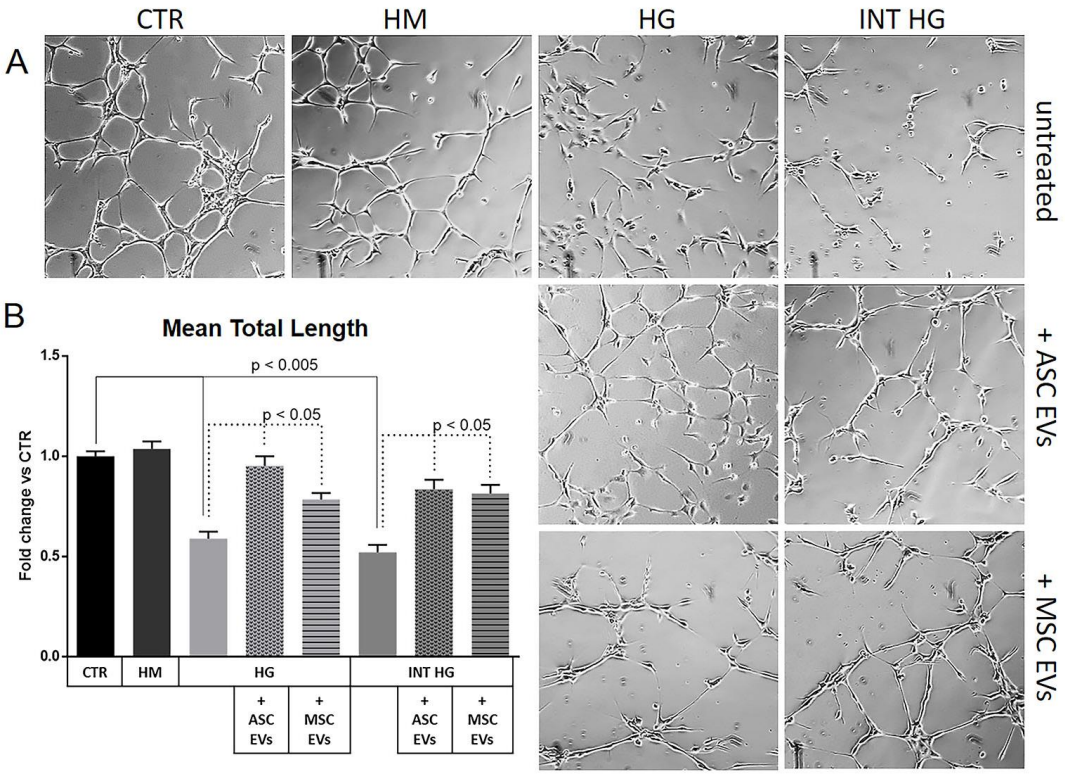

Figure 5: Pro-angiogenic activity of ASC and MSC EVs

Representative images of capillary-like structures formed by HMECs seeded on Matrigel-coated plates in different conditions: CTR, HM, HG, INT HG, HG + ASC EVs, INT HG + ASC EVs, HG + MSC EVs, INT HG + MSC EVs (A). Pictures were taken by a Leica camera installed on a Nikon inverted microscope at 10x magnification. Histograms show the mean total length ± SEM expressed as fold change over CTR for HG and INT HG models (B). N=4 experiments were performed for each data set. The statistical significance was calculated comparing HG/INT HG vs CTR and HG/INT HG + EVs vs HG/INT HG.

ASC and MSC EVs carry a common subset of miRNAs involved in angiogenesis and cell proliferation

To better understand if the biological effects previously described are due to the transfer of EV cargo to recipient cells, we performed miRNA and protein array characterization of ASC and MSC EVs. MiRNA screening was performed by qRT-PCR array. ASC and MSC EVs shown to carry 174 and 130 miRNAs respectively. The 20 most expressed miRNAs for each type of EVs were matched using Funrich. Seven miRNAs were present in both EVs (Fig. 6A), as well as three tRNA fragments (miR-1274a, miR-1274b, and miR-720, data not shown).

The gene enrichment analysis for the biological pathways targeted by the seven common miRNAs were performed by Funrich. Several biological pathways involved in regulation of cell proliferation (ErbB, PI3k, TGF-β signaling pathway) or angiogenesis (PDGF, VEGF, c-MET signaling pathway) and cell migration (Integrin and E-cadherin signaling) were significantly enriched (Fig. 6B). Then, by matching the seven miRNAs with the lists of miRNAs involved in KEGG or GO pathways regulating angiogenesis, cell cycle and apoptosis, we observed that all miRNAs are listed in one or more pathways (Fig. 6C). Moreover, the biological process enrichment analysis showed that the miRNAs are mostly involved in signal transduction, cell communication and cell growth (Fig. 6D). Lastly, KEGG pathway enrichment analysis performed by miRpath confirmed an enrichment in cell cycle, TGF-β, adherens junction and focal adhesion pathways (Fig. 7E).

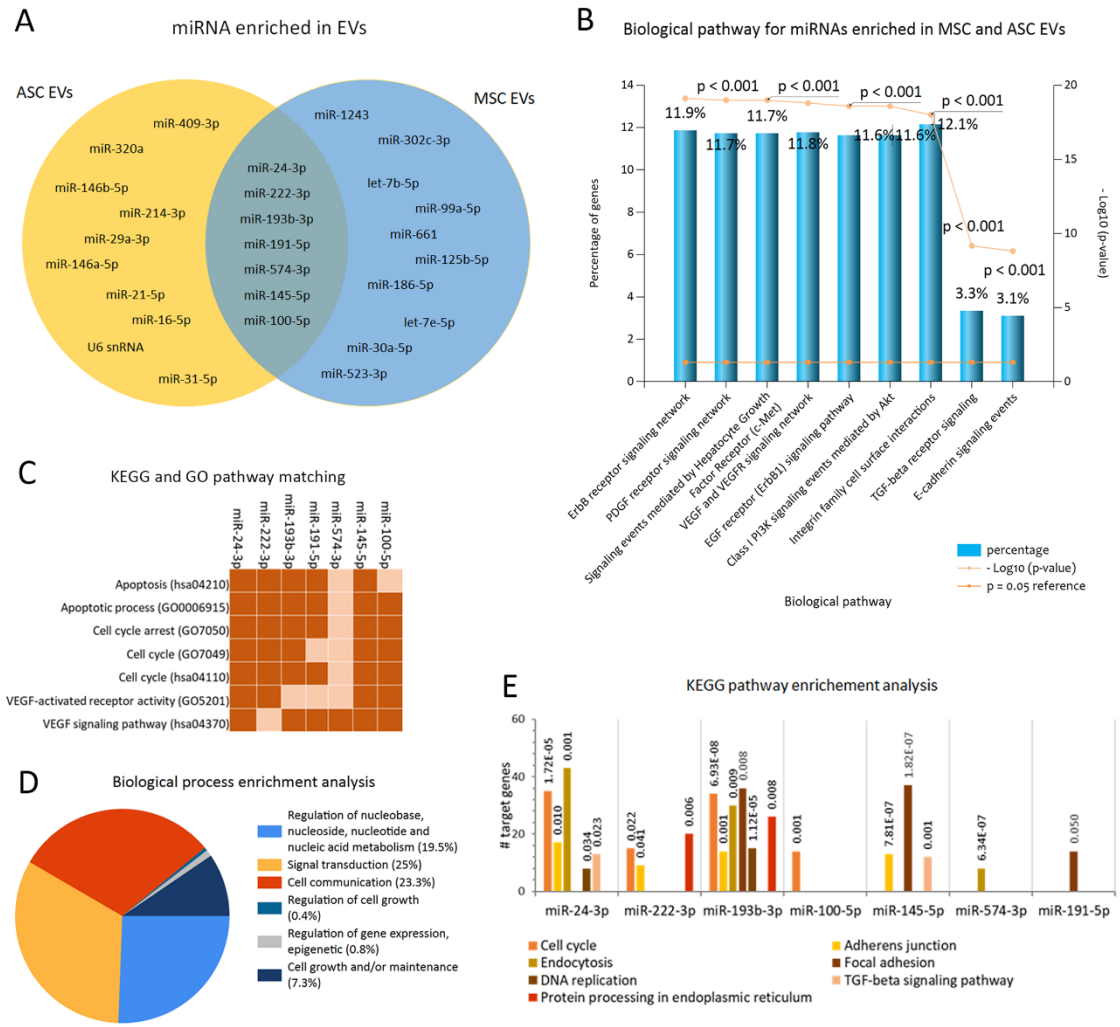

Figure 6: Bioinformatic analysis of ASC and MSC EVs common miRNA cargo

(**A**) The Venn diagram shows Funrich analysis of 17 miRNAs most enriched in ASC (yellow circle) and MSC (blue circle) EVs and 7 miRNAs expressed by both EVs (intersection) and used for the enrichment analysis. (**B**) The bar graph shows Funrich biological pathway enrichment analysis. X axis reports significantly enriched pathways, y axis reports the corresponding percentage of target genes (left) and -Log10(p-value) (right). (**C**) The clustergram represents the presence (dark orange) or absence (light orange) of each miRNA in each KEGG or GO pathway listed on the left. (**D**) The pie chart represents the percentage of each biological process (listed on the right), significantly enriched according to Funrich enrichment analysis. (**E**) The graph shows KEGG pathway enrichment analysis by miRpath. The bars represent the number of target genes for each miRNA (x axis) in each pathway and the respective p value. The legend below shows the color assigned to each pathway. The p value was calculated with FDR correction and threshold was set as 0.05.

ASC and MSC EVs carry a common subset of proteins involved in cell proliferation and apoptosis

Protein screening was performed by biotin label-based antibody array. By matching 79 proteins abundantly carried by ASC EVs and 62 proteins carried by MSC EVs, we detected 38 proteins common to both EVs (Fig. 7A). By Funrich enrichment analysis, we observed that this group of proteins significantly targets several pathways involved in cell adhesion (integrin, nectin), cell cycle or survival (PI3K, TGF-β, SMAD2/3), and angiogenesis (EGF receptor, cMET, VEGF) (Fig. 7B). Panther pathway enrichment analysis showed a significant involvement in TGF-β and PI3K signaling pathway, as well as interleukin, chemokine and cytokine signaling pathways (Fig. 7C). TGF-β signaling pathway enrichment was confirmed by GO biological process analysis performed by Enrichr. In addition, the latter analysis highlighted the positive regulation of cell proliferation, STAT and SMAD signaling, cell remodeling, but also the negative regulation of apoptosis (Fig. 7D).

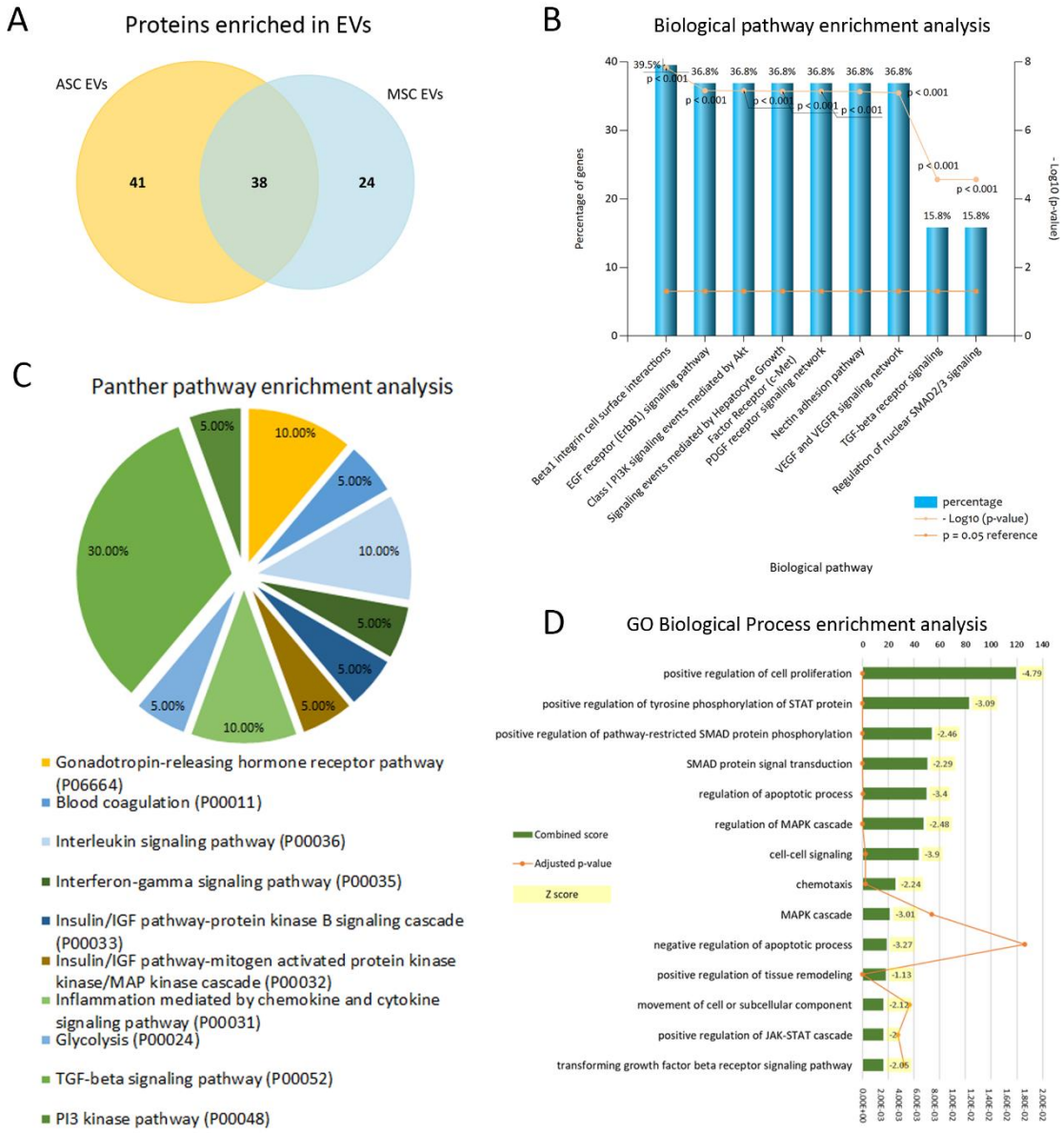

Figure 7: Bioinformatic analysis of ASC and MSC EV protein cargo

(**A**) The Venn diagram shows Funrich analysis of proteins most enriched in ASC (yellow circle) and MSC (blue circle) EVs. 38 proteins were present in both EVs (intersection) and were used for the enrichment analysis. (**B**) The bar graph shows Funrich biological pathway enrichment analysis. X axis reports significantly enriched pathways, y axis reports the respective percentage of target genes (left) and -Log10(p-value) (right). (**C**) The pie chart represents significantly enriched pathway (listed in legend) and the percentage of gene hit against total number of Pathway hits, according to Panther enrichment analysis. (**D**) The graph shows GO biological process enrichment analysis by Enrichr. Bars represent the combined score (upper x axis) for each biological process (y axis) and the respective adjusted p value (lower x axis).

ASC EVs miRNA and protein cargo targets common pathways involved in angiogenesis, cell motility and cell proliferation

Biological pathway enrichment analysis for miRNA most expressed in ASC EVs, but not present in MSC EVs, performed by Funrich, showed a statistically significant enrichment for pathways involved in angiogenesis (EGFR, c-MET, VEGF, PDGF, ErbB signaling pathways) and cell motility and/or adhesion to ECM (Nectin adhesion and integrin signaling pathways) (Fig. 8A). The same analysis was performed for the 41 proteins carried by ASC EVs, but not by MSC EVs. Interestingly, several pathways involved in angiogenesis and cell adhesion to ECM targeted by miRNAs were targeted also by proteins (Fig. 8B). KEGG pathway enrichment analysis for miRNAs performed by miRpath detected pathways involved in cell motility and adhesion (adherens junction, ECM receptor interactions, focal adhesion) and cell cycle and survival (cell cycle, TGF-β, Toll-like receptors signaling) (Fig. 8C). On the other hand, protein pathway analysis by Panther showed an enrichment in angiogenesis and apoptosis pathways, TGF-β, FGF, PDGF and Wnt signaling pathways (Fig. 8D). Lastly, GO biological process enrichment analysis performed by Enrichr detected the negative regulation of apoptotic process, and the positive regulation of ERK, PI3K, MAPK, JUN, and FGF pathways, all involved in cell cycle regulation and survival (Fig. 8E).

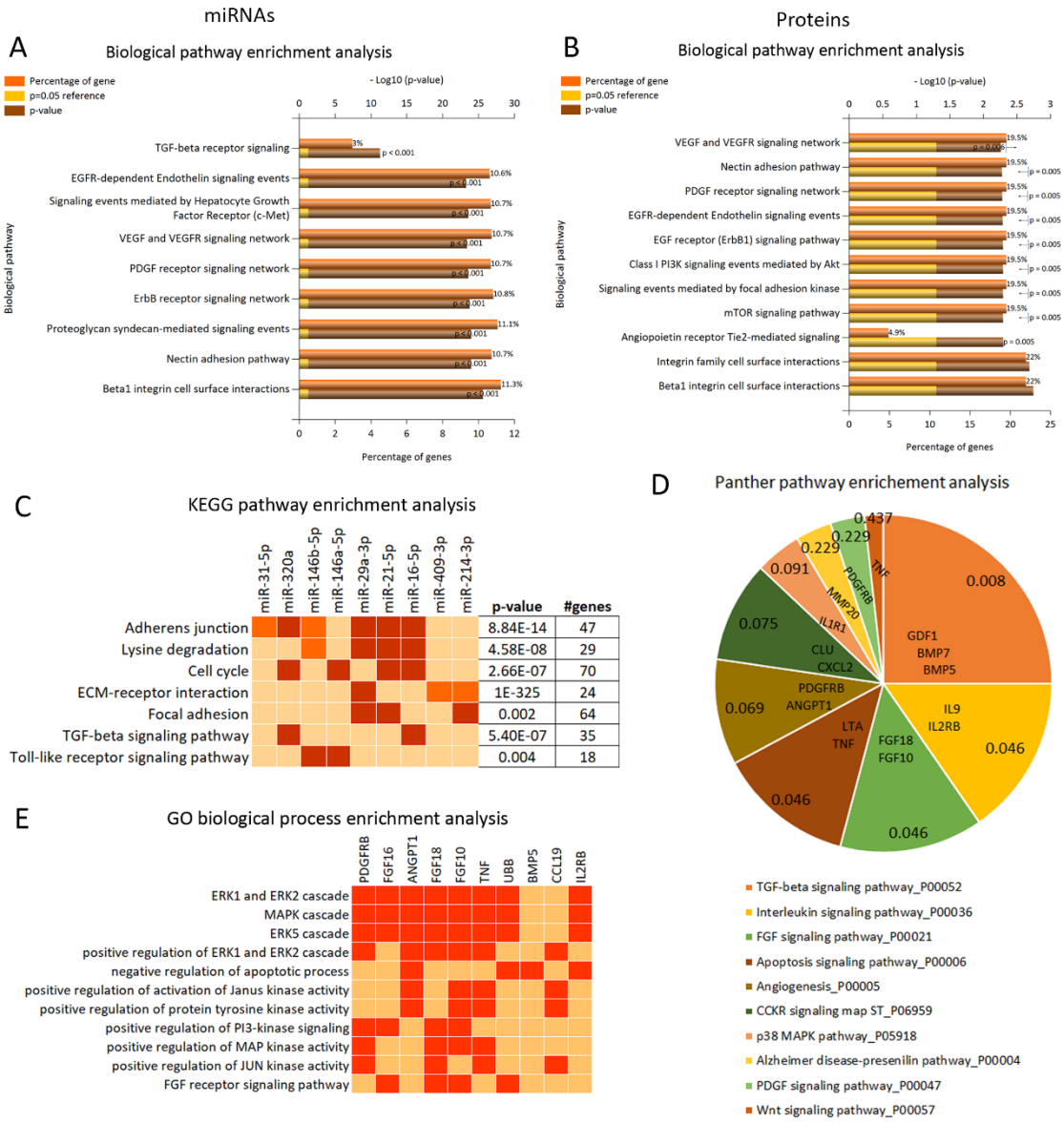

Figure 8: Bioinformatic analysis of ASC EV miRNA and protein cargo

Funrich biological pathway enrichment analysis for 9 miRNAs (**A**) and 41 proteins (**B**) exclusively carried by ASC EVs. The bar graphs show significantly enriched pathways (y axis), the respective percentage of target genes (lower x axis) and -Log10 (p-value) (upper x axis). (**C**) The clustergram represents KEGG pathway enriched (high target number=red, low target number=dark orange) or not (light orange), for each miRNA according to miRpath analysis. (**D**) The pie chart displays significantly enriched pathway (listed in legend), the involved proteins and the p value, according to Panther enrichment analysis. (**E**) The clustergram shows GO biological process enriched (red) or not (light orange) for each protein listed above according to Enrichr analysis.

MSC EVs miRNA and protein cargo targets common pathways involved in cell proliferation and endothelial cell migration

MiRNAs, most expressed in MSC EVs but not present in ASC EVs, were analyzed by Funrich. We observed a statistically significant enrichment for biological pathways involved in cell proliferation or survival (PI3K, TGF-β pathways), cell motility and/or adhesion to ECM (nectin, integrin and proteoglycan-syndecan signaling pathways) and angiogenesis (EGFR, c-MET, VEGF, PDGF, ErbB signaling pathways) (Fig. 9A). A second analysis performed by miRpath showed an enrichment for KEGG pathways involved in adhesion and motility (adherens junction, regulation of actin cytoskeleton, Wnt pathway), cell proliferation (cell cycle, DNA replication, mTOR, TGF-β, Wnt pathways), energy and metabolism (AMPK, FoxO, mTOR, HIF-1 pathways) (Fig. 9C). On the other hand, we performed the Funrich biological pathway analysis for the 24 proteins carried exclusively by MSC EVs. We observed an enrichment for the same pathways involved in cell adhesion and motility enriched in miRNA analysis (nectin, integrin and proteoglycan-syndecan signaling pathways), but also in pathways specific for the regulation of endothelial cell motility (endothelin and S1P1 pathways). Moreover, we observed a significant enrichment in pathways involved in angiogenesis and cell cycle (VEGF, PDGF, EGF, HIF-1 signaling, PI3K/AKT and mTOR pathways) (Fig. 9B). Panther pathway analysis confirmed the association with angiogenesis (angiogenesis, EGFR and PDGF pathways) and adhesion (cadherin and integrin signaling), as well as energy metabolism (fructose metabolism and glycolysis) and inflammation processes (Fig.9D). GO biological process analysis by Enrichr confirmed the positive involvement in cell proliferation, positive regulation of cell migration, ECM

interactions, angiogenesis-related pathways (VEGF, PDGF, EGF, c-MET signaling), tyrosine-kinase signaling and inflammation (Fig. 9E).

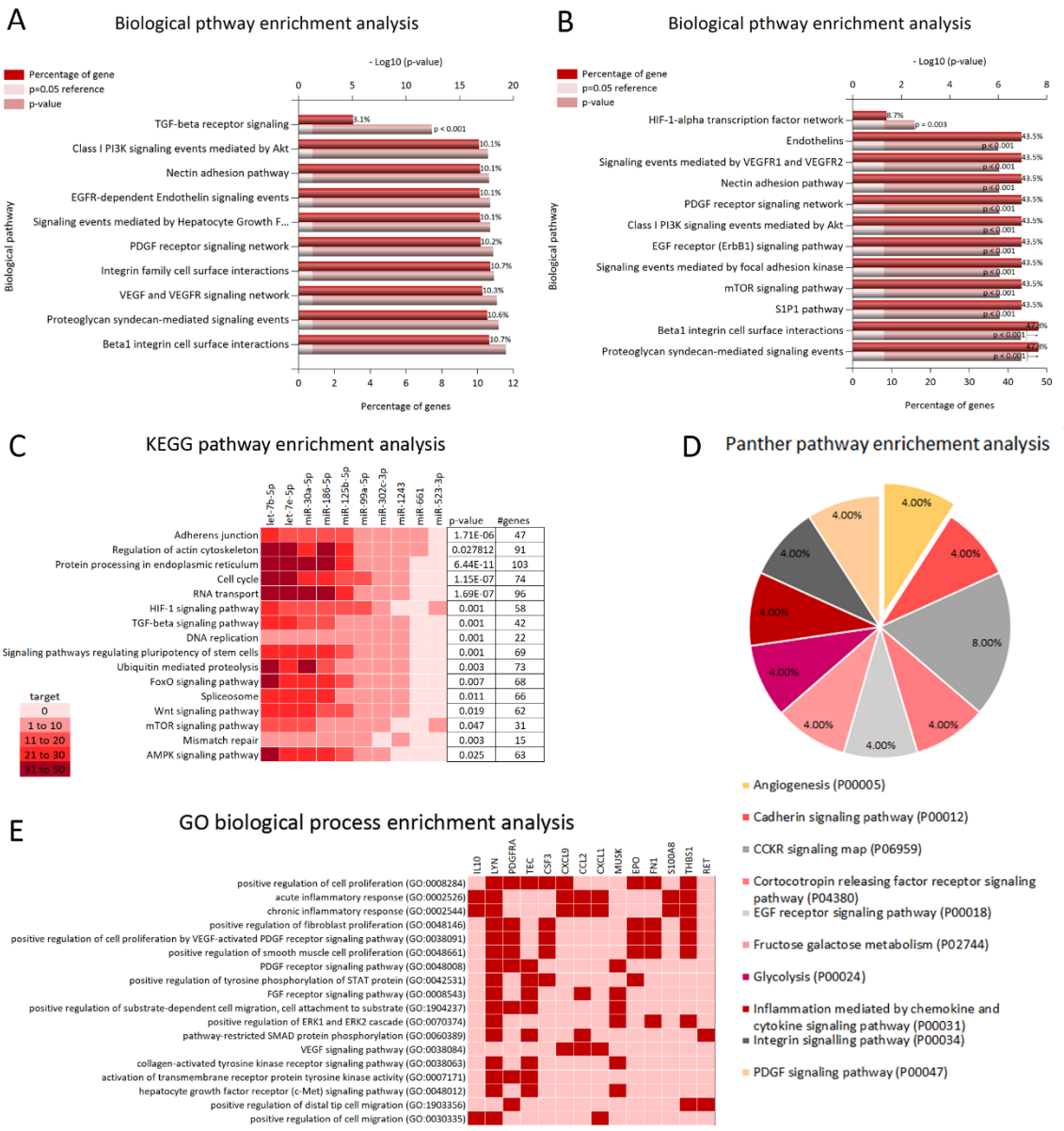

Figure 9: Bioinformatic analysis of MSC EV miRNA and protein cargo

Funrich biological pathway enrichment analysis for 9 miRNAs (**A**) and 24 proteins (**B**) exclusively carried by MSC EVs. The bar graphs show significantly enriched pathways (y axis), the respective percentage of target genes (lower x axis) and -Log10 (p-value) (upper x axis). (**C**) The clustergram represents KEGG pathway enriched, for each miRNA according to miRpath analysis. The color legend shows the respective number of targets for each color. (**D**) The pie chart displays significantly enriched pathway (listed in legend), and the percentage of gene hit against total number of Pathway hits, according to Panther enrichment analysis. (**E**) The clustergram shows GO biological process enriched (red) or not (pink) for each protein listed above, according to Enrichr analysis.

DISCUSSION

Chronic hyperglycemia can alter endothelial homeostasis and is a leading cause of endothelial disruption at the basis of several vascular injuries occurring in diabetes. The aim of our work was to test whether the known regenerative properties of stem cell-derived EVs were applicable in reverting endothelial damages induced by chronic hyperglycemia. Thus, we conditioned endothelial cells with a glucose concentration comparable to that measurable in diabetic patients. Cells were treated for 7 days, in order to mimic a chronic damage. At day 7 of HG or INT HG conditioning, we observed a statistically significant increase of fibronectin and v-CAM1 proteins. Fibronectin is a glycoprotein of the extracellular matrix that binds to integrins and plays a major role in cell adhesion, growth, migration, and wound healing. Increased fibronectin expression is associated with fibrosis and endothelial inflammation [108]. v-CAM1 is a vascular cell adhesion protein that mediates the adhesion of lymphocytes, monocytes, eosinophils and basophils to vascular endothelium. Upregulation of v-CAM1 in endothelial cells is associated to the development of atherosclerosis and endothelial inflammation [109]. Therefore, the upregulation of these proteins indicates that both HG and INT HG conditionings induced an inflammatory phenotype on endothelial cells. Moreover, we observed a statistically significant reduction of VEGF at both transcriptional and protein levels. VEGF is a signal protein that stimulates vasculogenesis and angiogenesis. Evidence shows that VEGF is downregulated in endothelial cells in hyperglycemic conditions and this stimulates cell apoptosis [110]. Moreover, VEGF reduction may lead to reduced vessel-structure formation ability and increased apoptosis. This confirms

that both HG and INT HG models were able to damage endothelial cells and were suitable *in vitro* models of hyperglycemic injury.

Then we observed that each hyperglycemic model induced both a reduction of the proliferation ability and an increase in the percentage of dead cells, in parallel to a reduction in the percentage of live cells. ASC and MSC EVs showed to antagonize high glucose effects on endothelial cells by promoting proliferation and inhibiting cells death.

Another sign of cells injury induced by high glucose is the oxidative stress, with the formation of free radicals leading to protein oxidation. Thus, we evaluated the levels of oxidized proteins in the hyperglycemic model before and after EV treatment. ASC and MSC EVs showed to promote a statistically significant reduction of oxidized proteins, whose levels were increased in hyperglycemic conditions. Consistent with our previous data [111], the present results suggest that EVs may play an anti-oxidant role.

Moreover, we observed that ASC and MSC EVs were able to restore the tube formation ability that was lost in HG and INT HG conditions. This confirms previous observations [72, 10] that ASC and MSC EVs have pro-angiogenic properties.

Finally, it is well known that EVs exert their biological effects by transferring their cargo to recipient cells [8, 7, 15, 57-61]. Therefore, we analyzed miRNA and protein cargo of ASC and MSC EVs and performed a bioinformatic analysis to better understand whether they carry molecules that can mediate the observed protective effects. Among miRNAs highly expressed by ASC and MSC EVs, we found seven that were present in both EV type. Biological, KEGG and GO pathway enrichment analysis showed a statistically significant enrichment for pathways involved in cell

cycle and proliferation, cell adhesion to ECM and angiogenesis, as well as apoptosis. The analysis of protein cargo revealed that ASC and MSC EVs shared 38 proteins. Interestingly, this group of proteins showed a significant enrichment in the same pathways previously observed in miRNA analysis. In addition, an enrichment in intracellular signaling pathways involved in signal transduction and regulation of cell survival and proliferation (STAT, SMAD, MAPK cascade) and cell motility were observed. These results suggest that ASC and MSC EVs may share some pro-proliferative, anti-apoptotic and pro-angiogenic effects because they carry a common subset of miRNAs and proteins which may provide a synergic effect by targeting common pathways.

Moreover, the bioinformatic analysis was performed on miRNAs and proteins exclusively carried by ASC EVs (Fig. 8) or by MSC EVs (Fig. 9). Also in this case, we observed that both miRNA and protein cargo of both EVs significantly target common pathways related to angiogenesis, cell cycle and motility. Furthermore, the analysis performed with different software based on different databases confirmed the enrichment in the same or functionally overlapping pathways. In addition, MSC EVs miRNA and protein cargo showed to target HIF-1 signaling pathways, which can be involved in angiogenesis, but also in response to oxidative stress. Interestingly, MSC EV protein cargo showed to target cell metabolism-related pathways, such as glycolysis and fructose galactose metabolism, which may be altered in hyperglycemic conditions. By comparing results of GO biological process enrichment analysis of protein cargo specifically enriched in ASC or MSC EVs, ASC EVs cargo seems to regulate mainly intracellular signal-transduction cascade, while MSC EVs seem to regulate signal transduction at a tyrosine kinase

receptor level. However, all processes seem to lead to the same final effects of positive regulation of proliferation and negative regulation of apoptosis. In addition, the regulation of pathways involved in cell-adhesion or cell-ECM interaction may promote cell motility and cytoskeleton remodeling, which is essential for vessel formation and remodeling.

Both shared protein cargo and MSC EVs-enriched proteins showed a significant correlation with modulation of inflammatory response. This is not surprising, since several reports about the immunomodulatory effect of MSC EVs has been provided over years [112].

Furthermore, the analysis of the molecular content of EVs is consistent with previous findings that MSC and ASC EVs contain several pro-angiogenic factors [10, 72, 74-76, 85-87] and miRNAs [82-84, 113].

CONCLUSIONS

In conclusion, our work shows that ASC and MSC EVs both exert regenerative effects in a hyperglycemic model that mimics *in vitro* microangiopathy conditions occurring in diabetic patients. EVs promote endothelial proliferation and survival contrasting hyperglycemia-induced injury. In addition, by inhibiting oxidation of endothelial proteins and by promoting angiogenesis, EVs may reduce the pro-inflammatory effect of hyperglycemia [95, 108-110] and the impaired angiogenesis [94]. Moreover, the concordant results of bioinformatic analysis confirm that several miRNAs and proteins carried by ASC and MSC EVs can be responsible for the pro-angiogenic, anti-apoptotic and pro-proliferative effects observed *in vitro*. Moreover, the analysis provides novel information about the specific signaling pathways that may be targeted by EVs, even if an experimental validation should be performed to confirm the results.

REFERENCES

1) Lötvall J, Hill AF, Hochberg F, Buzás EI, Di Vizio D, Gardiner C, Gho YS, Kurochkin IV, Mathivanan S, Quesenberry P, et al. Minimal experimental requirements for definition of extracellular vesicles and their functions: a position statement from the International Society for Extracellular Vesicles. J Extracell Vesicles. 2014 Dec 22;3:26913. doi:10.3402/jev.v3.26913.

2) Chaput N, Théry C. Exosomes: immune properties and potential clinical implementations. Semin Immunopathol. 2011 Sep;33(5):419-40. doi: 10.1007/s00281-010-0233-9

3) Bobrie A, Colombo M, Raposo G, Théry C. Exosome secretion: molecular mechanisms and roles in immune responses. Traffic. 2011 Dec;12(12):1659-68. doi: 10.1111/j.1600-0854.2011.01225.x. Review.

4) Lee Y, El Andaloussi S, Wood MJ. Exosomes and microvesicles: extracellular vesicles for genetic information transfer and gene therapy. Hum Mol Genet. 2012 Oct 15;21(R1):R125-34. Review.

5) Ratajczak MZ, Kucia M, Jadczyk T, Greco NJ, Wojakowski W, Tendera M, Ratajczak J. Pivotal role of paracrine effects in stem cell therapies in regenerative medicine: can we translate stem cell-secreted paracrine factors and microvesicles into better therapeutic strategies? Leukemia. 2012 Jun;26(6):1166-73. doi: 10.1038/leu.2011.389. Review.

6) Ratajczak J, Miekus K, Kucia M, Zhang J, Reca R, Dvorak P, Ratajczak MZ. Embryonic stem cell-derived microvesicles reprogram hematopoietic progenitors: evidence for horizontal transfer of mRNA and protein delivery. Leukemia. 2006 May;20(5):847-56.

7) Deregibus MC, Cantaluppi V, Calogero R, Lo Iacono M, Tetta C, Biancone L, Bruno S, Bussolati B, Camussi G. Endothelial progenitor cell derived microvesicles activate an angiogenic program in endothelial cells by a horizontal transfer of mRNA. Blood. 2007 Oct 1;110(7):2440-8.

8) Valadi H, Ekström K, Bossios A, Sjöstrand M, Lee JJ, Lötvall JO. Exosome-mediated transfer of mRNAs and microRNAs is a novel mechanism of genetic exchange between cells. Nat Cell Biol. 2007 Jun;9(6):654-9.

9) Balaj L, Lessard R, Dai L, Cho YJ, Pomeroy SL, Breakefield XO, Skog J. Tumour microvesicles contain retrotransposon elements and amplified oncogene sequences. Nat Commun. 2011 Feb 1;2:180. doi: 10.1038/ncomms1180.

10) Lopatina T, Bruno S, Tetta C, Kalinina N, Porta M, Camussi G. Platelet-derived growth factor regulates the secretion of extracellular vesicles by adipose mesenchymal stem cells and enhances their angiogenic potential. Cell Commun Signal. 2014 Apr 11;12:26. doi: 10.1186/1478-811X-12-26.

11) Trams EG, Lauter CJ, Salem N Jr, Heine U. Exfoliation of membrane ecto-enzymes in the form of micro-vesicles. Biochim Biophys Acta. 1981 Jul 6;645(1):63-70.

12) Pan BT, Johnstone RM. Fate of the transferrin receptor during maturation of sheep reticulocytes in vitro: selective externalization of the receptor. Cell. 1983 Jul;33(3):967-78.

13) Harding C, Heuser J, Stahl P. Endocytosis and intracellular processing of transferrin and colloidal gold-transferrin in rat reticulocytes: demonstration of a pathway for receptor shedding. Eur J Cell Biol. 1984 Nov;35(2):256-63..

14) Yáñez-Mó M, Siljander PR, Andreu Z, Zavec AB, Borràs FE, Buzas EI, Buzas K, Casal E, Cappello F, Carvalho J, et al. Biological properties of extracellular vesicles and their physiological functions. J Extracell Vesicles. 2015 May 14;4:27066. doi: 10.3402/jev.v4.27066.

15) Ratajczak J, Wysoczynski M, Hayek F, Janowska-Wieczorek A, Ratajczak MZ. Membrane-derived microvesicles: important and underappreciated mediators of cell-to-cell communication. Leukemia. 2006 Sep;20(9):1487-95.

16) Théry C, Ostrowski M, Segura E. Membrane vesicles as conveyors of immune responses. Nat Rev Immunol. 2009 Aug;9(8):581-93. doi: 10.1038/nri2567.

17) El Andaloussi S, Lakhal S, Mäger I, Wood MJ. Exosomes for targeted siRNA delivery across biological barriers. Adv Drug Deliv Rev. 2013 Mar;65(3):391-7. doi: 10.1016/j.addr.2012.08.008.

18) Greening DW, Xu R, Ji H, Tauro BJ, Simpson RJ. A protocol for exosome isolation and characterization: evaluation of ultracentrifugation, density-gradient separation, and immunoaffinity capture methods. Methods Mol Biol. 2015;1295:179-209. doi: 10.1007/978-1-4939-2550-6_15.

19) Muralidharan-Chari V, Clancy J, Plou C, Romao M, Chavrier P, Raposo G, D'Souza-Schorey C. ARF6-regulated shedding of tumor cell-derived plasma membrane microvesicles. Curr Biol. 2009 Dec 1;19(22):1875-85. doi: 10.1016/j.cub.2009.09.059.

20) Tricarico C, Clancy J, D'Souza-Schorey C. Biology and biogenesis of shed microvesicles. Small GTPases. 2017 Oct 2;8(4):220-232. doi: 10.1080/21541248.2016.1215283.

21) Hugel B, Martínez MC, Kunzelmann C, Freyssinet JM. Membrane microparticles: two sides of the coin. Physiology (Bethesda). 2005 Feb;20:22-7. Review.

22) Dignat-George F, Boulanger CM. The many faces of endothelial microparticles. Arterioscler Thromb Vasc Biol. 2011 Jan;31(1):27-33. doi: 10.1161/ATVBAHA.110.218123. Review.

23) Abid Hussein MN, Nieuwland R, Hau CM, Evers LM, Meesters EW, Sturk A. Cell-derived microparticles contain caspase 3 in vitro and in vivo. J Thromb Haemost. 2005 May;3(5):888-96.

24) Cocucci E, Racchetti G, Meldolesi J. Shedding microvesicles: artefacts no more. Trends Cell Biol. 2009 Feb;19(2):43-51. doi: 10.1016/j.tcb.2008.11.003. Review.

25) Mathivanan S, Ji H, Simpson RJ. Exosomes: extracellular organelles important in intercellular communication. J Proteomics. 2010 Sep 10;73(10):1907-20. doi: 10.1016/j.jprot.2010.06.006. Review.

26) György B, Szabó TG, Pásztói M, Pál Z, Misják P, Aradi B, László V, Pállinger E, Pap E, Kittel A, et al. Membrane vesicles, current state-of-the-art: emerging role of extracellular vesicles. Cell Mol Life Sci. 2011 Aug;68(16):2667-88. doi: 10.1007/s00018-011-0689-3. Review.

27) Juan T, Fürthauer M. Biogenesis and function of ESCRT-dependent extracellular vesicles. Semin Cell Dev Biol. 2017 Aug 12. pii: S1084-9521(17)30252-5. doi: 10.1016/j.semcdb.2017.08.022. Review.

28) Akers JC, Gonda D, Kim R, Carter BS, Chen CC. Biogenesis of extracellular vesicles (EV): exosomes, microvesicles, retrovirus-like vesicles, and apoptotic bodies. J Neurooncol. 2013 May;113(1):1-11. doi: 10.1007/s11060-013-1084-8.

29) Kowal J, Tkach M, Théry C. Biogenesis and secretion of exosomes. Curr Opin Cell Biol. 2014 Aug;29:116-25. doi: 10.1016/j.ceb.2014.05.004. Review.

30) Hyenne V, Apaydin A, Rodriguez D, Spiegelhalter C, Hoff-Yoessle S, Diem M, Tak S, Lefebvre O, Schwab Y, Goetz JG, Labouesse M. RAL-1 controls multivesicular body biogenesis and exosome secretion. J Cell Biol. 2015 Oct 12;211(1):27-37. doi: 10.1083/jcb.201504136.

31) Abels ER, Breakefield XO. Introduction to Extracellular Vesicles: Biogenesis, RNA Cargo Selection, Content, Release, and Uptake. Cell Mol Neurobiol. 2016 Apr;36(3):301-12. doi: 10.1007/s10571-016-0366-z. Review.

32) Zhang Y, Liu D, Chen X, Li J, Li L, Bian Z, Sun F, Lu J, Yin Y, Cai X, et al. Secreted monocytic miR-150 enhances targeted endothelial cell migration. Mol Cell. 2010 Jul 9;39(1):133-44. doi: 10.1016/j.molcel.2010.06.010.

33) Collino F, Deregibus MC, Bruno S, Sterpone L, Aghemo G, Viltono L, Tetta C, Camussi G. Microvesicles derived from adult human bone marrow and tissue specific mesenchymal stem cells shuttle selected pattern of miRNAs. PLoS One. 2010 Jul 27;5(7):e11803. doi: 10.1371/journal.pone.0011803.

34) Goldie BJ, Dun MD, Lin M, Smith ND, Verrills NM, Dayas CV, Cairns MJ. Activity-associated miRNA are packaged in Map1b-enriched exosomes released from depolarized neurons. Nucleic Acids Res. 2014 Aug;42(14):9195-208. doi: 10.1093/nar/gku594.

35) Li CC, Eaton SA, Young PE, Lee M, Shuttleworth R, Humphreys DT, Grau GE, Combes V, Bebawy M, Gong J, et al. Glioma microvesicles carry selectively packaged coding and non-coding RNAs which alter gene expression in recipient cells. RNA Biol. 2013 Aug;10(8):1333-44. doi: 10.4161/rna.25281.

36) Villarroya-Beltri C, Baixauli F, Gutiérrez-Vázquez C, Sánchez-Madrid F, Mittelbrunn M. Sorting it out: regulation of exosome loading. Semin Cancer Biol. 2014 Oct;28:3-13. doi: 10.1016/j.semcancer.2014.04.009. Review.

37) Iavello A, Frech VS, Gai C, Deregibus MC, Quesenberry PJ, Camussi G. Role of Alix in miRNA packaging during extracellular vesicle biogenesis. Int J Mol Med. 2016 Apr;37(4):958-66. doi: 10.3892/ijmm.2016.2488.

38) Melo SA, Sugimoto H, O'Connell JT, Kato N, Villanueva A, Vidal A, Qiu L, Vitkin E, Perelman LT, Melo CA, et al. Cancer exosomes perform cell-independent microRNA biogenesis and promote tumorigenesis. Cancer Cell. 2014 Nov 10;26(5):707-21. doi: 10.1016/j.ccell.2014.09.005.

39) Villarroya-Beltri C, Gutiérrez-Vázquez C, Sánchez-Cabo F, Pérez-Hernández D, Vázquez J, Martin-Cofreces N, Martinez-Herrera DJ, Pascual-Montano A, Mittelbrunn M, Sánchez-Madrid F. Sumoylated hnRNPA2B1 controls the sorting of miRNAs into exosomes through binding to specific motifs. Nat Commun. 2013;4:2980. doi:10.1038/ncomms3980.

40) Shurtleff MJ, Temoche-Diaz MM, Karfilis KV, Ri S, Schekman R. Y-box protein 1 is required to sort microRNAs into exosomes in cells and in a cell-free reaction. Elife. 2016 Aug 25;5. pii: e19276. doi: 10.7554/eLife.19276.

41) Cha DJ, Franklin JL, Dou Y, Liu Q, Higginbotham JN, Demory Beckler M, Weaver AM, Vickers K, Prasad N, Levy S, et al. KRAS-dependent sorting of miRNA to exosomes. Elife. 2015 Jul 1;4:e07197. doi: 10.7554/eLife.07197.

42) McKenzie AJ, Hoshino D, Hong NH, Cha DJ, Franklin JL, Coffey RJ, Patton JG, Weaver AM. KRAS-MEK Signaling Controls Ago2 Sorting into Exosomes. Cell Rep. 2016 May 3;15(5):978-987. doi: 10.1016/j.celrep.2016.03.085.

43) Tosar JP, Gámbaro F, Sanguinetti J, Bonilla B, Witwer KW, Cayota A. Assessment of small RNA sorting into different extracellular fractions revealed by high-throughput sequencing of breast cell lines. Nucleic Acids Res. 2015 Jun 23;43(11):5601-16. doi: 10.1093/nar/gkv432.

44) van Balkom BW, Eisele AS, Pegtel DM, Bervoets S, Verhaar MC. Quantitative and qualitative analysis of small RNAs in human endothelial cells and exosomes provides insights into localized RNA processing, degradation and sorting. J Extracell Vesicles. 2015 May 29;4:26760. doi: 10.3402/jev.v4.26760.

45) Nolte-'t Hoen EN, Buermans HP, Waasdorp M, Stoorvogel W, Wauben MH, 't Hoen PA. Deep sequencing of RNA from immune cell-derived vesicles uncovers the selective incorporation of small non-coding RNA biotypes with potential regulatory functions. Nucleic Acids Res. 2012 Oct;40(18):9272-85. doi: 10.1093/nar/gks658.

46) Lambertz U, Oviedo Ovando ME, Vasconcelos EJ, Unrau PJ, Myler PJ, Reiner NE. Small RNAs derived from tRNAs and rRNAs are highly enriched in exosomes from both old and new world Leishmania providing evidence for conserved exosomal RNA Packaging. BMC Genomics. 2015 Mar 5;16:151. doi: 10.1186/s12864-015-1260-7.

47) Miyanishi M, Tada K, Koike M, Uchiyama Y, Kitamura T, Nagata S. Identification of Tim4 as a phosphatidylserine receptor. Nature. 2007 Nov 15;450(7168):435-9.

48) Christianson HC, Svensson KJ, van Kuppevelt TH, Li JP, Belting M. Cancer cell exosomes depend on cell-surface heparan sulfate proteoglycans for their internalization and functional activity. Proc Natl Acad Sci U S A. 2013 Oct 22;110(43):17380-5. doi: 10.1073/pnas.1304266110.

49) Vargas A, Zhou S, Éthier-Chiasson M, Flipo D, Lafond J, Gilbert C, Barbeau B. Syncytin proteins incorporated in placenta exosomes are important for cell uptake and show variation in abundance in serum exosomes from patients with preeclampsia. FASEB J. 2014 Aug;28(8):3703-19. doi: 10.1096/fj.13-239053.

50) Mulcahy LA, Pink RC, Carter DR. Routes and mechanisms of extracellular vesicle uptake. J Extracell Vesicles. 2014 Aug 4;3. doi: 10.3402/jev.v3.24641. Review.

51) Maas SL, Breakefield XO, Weaver AM. Extracellular Vesicles: Unique Intercellular Delivery Vehicles. Trends Cell Biol. 2017 Mar;27(3):172-188. doi: 10.1016/j.tcb.2016.11.003. Review.

52) Gildea JJ, Seaton JE, Victor KG, Reyes CM, Bigler Wang D, Pettigrew AC, Courtner CE, Shah N, Tran HT, Van Sciver RE, Carlson JM, Felder RA. Exosomal transfer from human renal proximal tubule cells to distal tubule and collecting duct cells. Clin Biochem. 2014 Oct;47(15):89-94. doi: 10.1016/j.clinbiochem.2014.06.018.

53) Parolini I, Federici C, Raggi C, Lugini L, Palleschi S, De Milito A, Coscia C, Iessi E, Logozzi M, Molinari A, Colone M, Tatti M, Sargiacomo M, Fais S. Microenvironmental pH is a key factor for exosome traffic in tumor cells. J Biol Chem. 2009 Dec 4;284(49):34211-22. doi: 10.1074/jbc.M109.041152.

54) Yang C, Xiong W, Qiu Q, Shao Z, Hamel D, Tahiri H, Leclair G, Lachapelle P, Chemtob S, Hardy P. Role of receptor-mediated endocytosis in the antiangiogenic effects of human T lymphoblastic cell-derived microparticles. Am J Physiol Regul Integr Comp Physiol. 2012 Apr 15;302(8):R941-9. doi: 10.1152/ajpregu.00527.2011.

55) Barry OP, Praticò D, Savani RC, FitzGerald GA. Modulation of monocyte-endothelial cell interactions by platelet microparticles. J Clin Invest. 1998 Jul 1;102(1):136-44.

56) Janowska-Wieczorek A, Majka M, Kijowski J, Baj-Krzyworzeka M, Reca R, Turner AR, Ratajczak J, Emerson SG, Kowalska MA, Ratajczak MZ. Platelet-derived microparticles bind to hematopoietic stem/progenitor cells and enhance their engraftment. Blood. 2001 Nov 15;98(10):3143-9.

57) Skog J, Würdinger T, van Rijn S, Meijer DH, Gainche L, Sena-Esteves M, Curry WT Jr, Carter BS, Krichevsky AM, Breakefield XO. Glioblastoma microvesicles transport RNA and proteins that promote tumour growth and provide diagnostic biomarkers. Nat Cell Biol. 2008 Dec;10(12):1470-6. doi: 10.1038/ncb1800.

58) Zhang J, Li S, Li L, Li M, Guo C, Yao J, Mi S. Exosome and exosomal microRNA: trafficking, sorting, and function. Genomics Proteomics Bioinformatics. 2015 Feb;13(1):17-24. doi: 10.1016/j.gpb.2015.02.001.

59) Bruno S, Grange C, Deregibus MC, Calogero RA, Saviozzi S, Collino F, Morando L, Busca A, Falda M, Bussolati B, Tetta C, Camussi G. Mesenchymal stem cell-derived microvesicles protect against acute tubular injury. J Am Soc Nephrol. 2009 May;20(5):1053-67. doi: 10.1681/ASN.2008070798..

60) Aliotta JM, Pereira M, Johnson KW, de Paz N, Dooner MS, Puente N, Ayala C, Brilliant K, Berz D, Lee D, et al. Microvesicle entry into marrow cells mediates tissue-specific changes in mRNA by direct delivery of mRNA and induction of transcription. Exp Hematol. 2010 Mar;38(3):233-45. doi: 10.1016/j.exphem.2010.01.002.

61) Montecalvo A, Larregina AT, Shufesky WJ, Stolz DB, Sullivan ML, Karlsson JM, Baty CJ, Gibson GA, Erdos G, Wang Z, et al. Mechanism of transfer of functional microRNAs between mouse dendritic cells via exosomes. Blood. 2012 Jan 19;119(3):756-66. doi: 10.1182/blood-2011-02-338004.

62) Ridder K, Keller S, Dams M, Rupp AK, Schlaudraff J, Del Turco D, Starmann J, Macas J, Karpova D, Devraj K, et al. Extracellular vesicle-mediated transfer of genetic information between the hematopoietic system and the brain in response to inflammation. PLoS Biol. 2014 Jun 3;12(6):e1001874. doi: 10.1371/journal.pbio.1001874.

63) Ridder K, Sevko A, Heide J, Dams M, Rupp AK, Macas J, Starmann J, Tjwa M, Plate KH, Sültmann H, et al. Extracellular vesicle-mediated transfer of functional RNA in the tumor microenvironment. Oncoimmunology. 2015 Mar 19;4(6):e1008371.

64) Zomer A, Maynard C, Verweij FJ, Kamermans A, Schäfer R, Beerling E, Schiffelers RM, de Wit E, Berenguer J, Ellenbroek SIJ, et al. In Vivo imaging reveals extracellular vesicle-mediated phenocopying of metastatic behavior. Cell. 2015 May 21;161(5):1046-1057. doi: 10.1016/j.cell.2015.04.042.

65) Lai CP, Kim EY, Badr CE, Weissleder R, Mempel TR, Tannous BA, Breakefield XO. Visualization and tracking of tumour extracellular vesicle delivery and RNA translation using multiplexed reporters. Nat Commun. 2015 May 13;6:7029. doi: 10.1038/ncomms8029.

66) Miyamoto S, Kowalska MA, Marcinkiewicz C, Marcinkiewicz MM, Mosser D, Edmunds LH Jr, Niewiarowski S. Interaction of leukocytes with platelet microparticles derived from outdated platelet concentrates. Thromb Haemost. 1998 Dec;80(6):982-8.

67) Kassem M, Kristiansen M, Abdallah BM. Mesenchymal stem cells: cell biology and potential use in therapy. Basic Clin Pharmacol Toxicol. 2004 Nov; 95(5): 209-14. Review.

68) Kern S, Eichler H, Stoeve J, Klüter H, Bieback K. Comparative analysis of mesenchymal stem cells from bone marrow, umbilical cord blood, or adipose tissue. Stem Cells. 2006 May;24(5):1294-301.

69) Dominici M, Le Blanc K, Mueller I, Slaper-Cortenbach I, Marini F, Krause D, Deans R, Keating A, Prockop Dj, Horwitz E. Minimal criteria for defining multipotent mesenchymal stromal cells. The International Society for Cellular Therapy position statement. Cytotherapy. 2006;8(4):315-7.

70) Rani S, Ryan AE, Griffin MD, Ritter T. Mesenchymal Stem Cell-derived Extracellular Vesicles: Toward Cell-free Therapeutic Applications. Mol Ther. 2015 May;23(5):812-823. doi: 10.1038/mt.2015.44. Review.

71) Biancone L, Bruno S, Deregibus MC, Tetta C, Camussi G. Therapeutic potential of mesenchymal stem cell-derived microvesicles. Nephrol Dial Transplant. 2012 Aug;27(8):3037-42. doi: 10.1093/ndt/gfs168. Review.

72) Merino-González C, Zuñiga FA, Escudero C, Ormazabal V, Reyes C, Nova-Lamperti E, Salomón C, Aguayo C. Mesenchymal Stem Cell-Derived Extracellular Vesicles Promote Angiogenesis: Potencial Clinical Application. Front Physiol. 2016 Feb 9;7:24. doi: 10.3389/fphys.2016.00024. Review.

73) Dai R, Wang Z, Samanipour R, Koo KI, Kim K. Adipose-Derived Stem Cells for Tissue Engineering and Regenerative Medicine Applications. Stem Cells Int. 2016;2016:6737345. doi: 10.1155/2016/6737345. Review.

74) Coultas L, Chawengsaksophak K, Rossant J. Endothelial cells and VEGF in vascular development. Nature. 2005 Dec 15;438(7070):937-45. Review.

75) Olsson AK, Dimberg A, Kreuger J, Claesson-Welsh L. VEGF receptor signalling - in control of vascular function. Nat Rev Mol Cell Biol. 2006 May;7(5):359-71. Review.

76) Morishita R, Nakamura S, Hayashi S, Taniyama Y, Moriguchi A, Nagano T, Taiji M, Noguchi H, Takeshita S, Matsumoto K, Nakamura T, Higaki J, Ogihara T. Therapeutic angiogenesis induced by human recombinant hepatocyte growth factor in rabbit hind limb ischemia model as cytokine supplement therapy. Hypertension. 1999 Jun;33(6):1379-84.

77) Chade AR, Stewart N. Angiogenic cytokines in renovascular disease: do they have potential for therapeutic use? J Am Soc Hypertens. 2013 Mar-Apr;7(2):180-90. doi: 10.1016/j.jash.2013.01.004. Review.

78) Tan CY, Lai RC, Wong W, Dan YY, Lim SK, Ho HK. Mesenchymal stem cell-derived exosomes promote hepatic regeneration in drug-induced liver injury models. Stem Cell Res Ther. 2014 Jun 10;5(3):76. doi: 10.1186/scrt465.

79) Kitagawa M, Hojo M, Imayoshi I, Goto M, Ando M, Ohtsuka T, Kageyama R, Miyamoto S. Hes1 and Hes5 regulate vascular remodeling and arterial specification of endothelial cells in brain vascular development. Mech Dev. 2013 Sep-Oct;130(9-10):458-66. doi: 10.1016/j.mod.2013.07.001.

80) Maruotti N, Corrado A, Neve A, Cantatore FP. Systemic effects of Wnt signaling. J Cell Physiol. 2013 Jul;228(7):1428-32. doi: 10.1002/jcp.24326. Review.

81) Lu R, Qu Y, Ge J, Zhang L, Su Z, Pflugfelder SC, Li DQ. Transcription factor TCF4 maintains the properties of human corneal epithelial stem cells. Stem Cells. 2012 Apr;30(4):753-61. doi: 10.1002/stem.1032.

82) Chen TS, Lai RC, Lee MM, Choo AB, Lee CN, Lim SK. Mesenchymal stem cell secretes microparticles enriched in pre-microRNAs. Nucleic Acids Res. 2010 Jan;38(1):215-24. doi: 10.1093/nar/gkp857.

83) Yoo JK, Kim J, Choi SJ, Noh HM, Kwon YD, Yoo H, Yi HS, Chung HM, Kim JK. Discovery and characterization of novel microRNAs during endothelial differentiation of human embryonic stem cells. Stem Cells Dev. 2012 Jul 20;21(11):2049-57. doi: 10.1089/scd.2011.0500.

84) Nagpal N, Kulshreshtha R. miR-191: an emerging player in disease biology. Front Genet. 2014 Apr 23;5:99. doi: 10.3389/fgene.2014.00099. Review.

85) Lee JK, Park SR, Jung BK, Jeon YK, Lee YS, Kim MK, Kim YG, Jang JY, Kim CW. Exosomes derived from mesenchymal stem cells suppress angiogenesis by down-regulating VEGF expression in breast cancer cells. PLoS One. 2013 Dec 31;8(12):e84256. doi: 10.1371/journal.pone.0084256.

86) Lopatina T, Mazzeo A, Bruno S, Tetta C, Kalinina N, et al. The angiogenic potential of adipose mesenchymal stem cell-derived extracellular vesicles is modulated by basic fibroblast growth factor. J Stem Cell Res Ther 2014 4(10): 245. doi:10.4172/2157-7633.1000245.

87) Togliatto G, Dentelli P, Gili M, Gallo S, Deregibus C, Biglieri E, Iavello A, Santini E, Rossi C, Solini A, Camussi G, Brizzi MF. Obesity reduces the pro-angiogenic potential of adipose tissue stem cell-derived extracellular vesicles (EVs) by impairing miR-126 content: impact on clinical applications. Int J Obes (Lond). 2016 Jan;40(1):102-11. doi: 10.1038/ijo.2015.123.

88) Collino F, Bruno S, Incarnato D, Dettori D, Neri F, Provero P, Pomatto M, Oliviero S, Tetta C, Quesenberry PJ, Camussi G. AKI Recovery Induced by Mesenchymal Stromal Cell-Derived Extracellular Vesicles Carrying MicroRNAs. J Am Soc Nephrol. 2015 Oct;26(10):2349-60. doi: 10.1681/ASN.2014070710.

89) Zou X, Gu D, Xing X, Cheng Z, Gong D, Zhang G, Zhu Y. Human mesenchymal stromal cell-derived extracellular vesicles alleviate renal ischemic reperfusion injury and enhance angiogenesis in rats. Am J Transl Res. 2016 Oct 15;8(10):4289-4299.

90) Shabbir A, Cox A, Rodriguez-Menocal L, Salgado M, Van Badiavas E. Mesenchymal Stem Cell Exosomes Induce Proliferation and Migration of Normal and Chronic Wound Fibroblasts, and Enhance Angiogenesis In Vitro. Stem Cells Dev. 2015 Jul 15;24(14):1635-47. doi: 10.1089/scd.2014.0316.

91) Zhang J, Guan J, Niu X, Hu G, Guo S, Li Q, Xie Z, Zhang C, Wang Y. Exosomes released from human induced pluripotent stem cells-derived MSCs facilitate cutaneous wound healing by promoting collagen synthesis and angiogenesis. J Transl Med. 2015 Feb 1;13:49. doi: 10.1186/s12967-015-0417-0.

92) Bakker W, Eringa EC, Sipkema P, van Hinsbergh VW. Endothelial dysfunction and diabetes: roles of hyperglycemia, impaired insulin signaling and obesity. Cell Tissue Res. 2009 Jan;335(1):165-89. doi: 10.1007/s00441-008-0685-6.

93) Shi Y, Vanhoutte PM. Macro- and microvascular endothelial dysfunction in diabetes. J Diabetes. 2017 May;9(5):434-449. doi: 10.1111/1753-0407.12521.

94) Schalkwijk CG, Stehouwer CD. Vascular complications in diabetes mellitus: the role of endothelial dysfunction. Clin Sci (Lond). 2005 Aug;109(2):143-59.

95) di Mario U, Pugliese G. Pathogenetic mechanisms of diabetic microangiopathy. International Congress Series. 20031253:171-182.

96) Rask-Madsen C, King GL. Vascular complications of diabetes: mechanisms of injury and protective factors. Cell Metab. 2013 Jan 8;17(1):20-33. doi:10.1016/j.cmet.2012.11.012.

97) Ades EW, Candal FJ, Swerlick RA, George VG, Summers S, Bosse DC, Lawley TJ. HMEC-1: establishment of an immortalized human microvascular endothelial cell line. J Invest Dermatol. 1992 Dec;99(6):683-90.

98) Xu Y, Swerlick RA, Sepp N, Bosse D, Ades EW, Lawley TJ. Characterization of expression and modulation of cell adhesion molecules on an immortalized human dermal microvascular endothelial cell line (HMEC-1). J Invest Dermatol. 1994 Jun;102(6):833-7.

99) Zanone MM, Favaro E, Conaldi PG, Greening J, Bottelli A, Perin PC, Klein NJ, Peakman M, Camussi G. Persistent infection of human microvascular endothelial cells by coxsackie B viruses induces increased expression of adhesion molecules. J Immunol. 2003 Jul 1;171(1):438-46.

100) Dragovic RA, Gardiner C, Brooks AS, Tannetta DS, Ferguson DJ, Hole P, Carr B, Redman CW, Harris AL, Dobson PJ, Harrison P, Sargent IL. Sizing and phenotyping of cellular vesicles using Nanoparticle Tracking Analysis. Nanomedicine. 2011 Dec;7(6):780-8. doi: 10.1016/j.nano.2011.04.003.

101) Burgess A, Vigneron S, Brioudes E, Labbé JC, Lorca T, Castro A. Loss of human Greatwall results in G2 arrest and multiple mitotic defects due to deregulation of the cyclin B-Cdc2/PP2A balance. Proc Natl Acad Sci U S A. 2010 Jul 13;107(28):12564-9. doi: 10.1073/pnas.0914191107.

102) McCloy RA, Rogers S, Caldon CE, Lorca T, Castro A, Burgess A. Partial inhibition of Cdk1 in G 2 phase overrides the SAC and decouples mitotic events. Cell Cycle. 2014;13(9):1400-12. doi: 10.4161/cc.28401.

103) Mestdagh P, Van Vlierberghe P, De Weer A, Muth D, Westermann F, Speleman F, Vandesompele J. A novel and universal method for microRNA RT-qPCR data normalization. Genome Biol. 2009;10(6):R64. doi: 10.1186/gb-2009-10-6-r64.

104) Pathan M, Keerthikumar S, Ang CS, Gangoda L, Quek CY, Williamson NA, Mouradov D, Sieber OM, Simpson RJ, Salim A, et al. FunRich: An open access standalone functional enrichment and interaction network analysis tool. Proteomics. 2015 Aug;15(15):2597-601. doi: 10.1002/pmic.201400515.

105) Vlachos IS, Zagganas K, Paraskevopoulou MD, Georgakilas G, Karagkouni D, Vergoulis T, et al. DIANA-miRPath v3.0: deciphering microRNA function with experimental support. Nucleic Acids Res 2015;43(1):460-6.

106) Chen EY, Tan CM, Kou Y, Duan Q, Wang Z, Meirelles GV, Clark NR, Ma'ayan A. Enrichr: interactive and collaborative HTML5 gene list enrichment analysis tool. BMC Bioinformatics. 2013 Apr 15;14:128. doi: 10.1186/1471-2105-14-128.

107) Kuleshov MV, Jones MR, Rouillard AD, Fernandez NF, Duan Q, Wang Z, Koplev S, Jenkins SL, Jagodnik KM, Lachmann A, et al. Enrichr: a comprehensive gene set enrichment analysis web server 2016 update. Nucleic Acids Research. 2016 Jul 8;44(W1):W90-7. doi: 10.1093/nar/gkw377.

108) Feaver RE, Gelfand BD, Wang C, Schwartz MA, Blackman BR. Atheroprone hemodynamics regulate fibronectin deposition to create positive feedback that sustains endothelial inflammation. Circ Res. 2010 Jun 11;106(11):1703-11. doi:10.1161/CIRCRESAHA.109.216283.

109) Verginelli F, Adesso L, Limon I, Alisi A, Gueguen M, Panera N, Giorda E, Raimondi L, Ciarapica R, Campese AF, et al. Activation of an endothelial Notch1-Jagged1 circuit induces VCAM1 expression, an effect amplified by interleukin-1β. Oncotarget. 2015 Dec 22;6(41):43216-29. doi: 10.18632/oncotarget.6456.

110) Yang Z, Mo X, Gong Q, Pan Q, Yang X, Cai W, Li C, Ma JX, He Y, Gao G. Critical effect of VEGF in the process of endothelial cell apoptosis induced by high glucose. Apoptosis. 2008 Nov;13(11):1331-43. doi: 10.1007/s10495-008-0257-y.

111) Gallo S, Gili M, Lombardo G, Rossetti A, Rosso A, Dentelli P, Togliatto G, Deregibus MC, Taverna D, Camussi G, Brizzi MF. Stem Cell-Derived, microRNA-Carrying Extracellular Vesicles: A Novel Approach to Interfering with Mesangial Cell Collagen Production in a Hyperglycaemic Setting. PLoS One. 2016 Sep 9;11(9):e0162417. doi: 10.1371/journal.pone.0162417.

112) Burrello J, Monticone S, Gai C, Gomez Y, Kholia S, Camussi G. Stem Cell-Derived Extracellular Vesicles and Immune-Modulation. Front Cell Dev Biol. 2016 Aug 22;4:83. doi: 10.3389/fcell.2016.00083. Review.

113) Collino F, Pomatto M, Bruno S, Lindoso RS, Tapparo M, Sicheng W, Quesenberry P, Camussi G. Exosome and Microvesicle-Enriched Fractions Isolated from Mesenchymal Stem Cells by Gradient Separation Showed Different Molecular Signatures and Functions on Renal Tubular Epithelial Cells. Stem Cell Rev. 2017 Apr;13(2):226-243. doi: 10.1007/s12015-016-9713-1.